

SIGNATURE AND CONCORDANCE OF VIRTUAL KNOTS

HANS U. BODEN, MICAH CHRISMAN, AND ROBIN GAUDREAU

ABSTRACT. We introduce signature invariants of virtual knots and use them to investigate virtual knot concordance. The signatures, which depend on a choice of Seifert surface, are defined first for almost classical knots and then extended to all virtual knots using parity projection and Turaev’s coverings of knots. A key step is a result implying that parity projection preserves concordance of virtual knots. One obtains similar results for long virtual knots, and in this case the knot signature is seen to be independent of the choice of Seifert surface.

In addition to the knot signatures, we use the Seifert pairing to define several other invariants for almost classical knots, including the Alexander-Conway polynomials, the nullity, the ω -signatures, and the directed Alexander polynomials. These invariants are applied to the problem of determining the slice genus for almost classical knots. There are 76 almost classical knots with up to six crossings, and we determine the slice status for all of them and the slice genus for all but four. These results are summarized in Table 2.

INTRODUCTION

Virtual knots were introduced by Kauffman in [Kau99], and many classical invariants such as the knot group and the Jones polynomial extend in a straightforward way. Virtual knots can be viewed geometrically as equivalence classes of knots in thickened surfaces up to stable equivalence [CKS02], and alternatively they can be represented combinatorially as Gauss diagrams up to Reidemeister moves (see Figure 1). Both points of view are useful and important. For instance, from the combinatorial approach virtual knots provide the natural setting for investigating finite-type invariants [GPV00].

Concordance and cobordism of virtual knots were introduced in [CKS02, Tur08, Kau15], and this aspect can be studied geometrically via a representative knot in a thickened surface (see Definition 1.1) or combinatorially via a representative Gauss diagram (see Figure 2).

Recent results in virtual knot concordance include the extension of Rasmussen’s invariant by Dye, Kaestner, and Kauffman [DKK17], which is based on Manturov’s generalization of Khovanov homology to virtual knots [Man07], and applications of Turaev’s graded genus to determining sliceness and the slice genus of low-crossing virtual knots [BCG17a]. However, our understanding of virtual knot concordance is still quite limited, and very few virtual knot invariants are known to be invariant under virtual knot concordance.

One of the most important concordance invariants for classical knots is the knot signature. This invariant is usually defined in terms of the Seifert pairing as the signature of $V + V^\tau$, the symmetrized Seifert matrix. This is possible because every classical knot admits a Seifert surface. To show that it is well-defined, notice that the S -equivalence class of the Seifert matrix is independent of the choice of Seifert surface and $\text{sig}(V + V^\tau)$ depends only on the S -equivalence class of V . None of these results are true for virtual knots; Seifert surfaces

Date: December 14, 2024.

2010 Mathematics Subject Classification. Primary: 57M25, Secondary: 57M27.

Key words and phrases. Virtual knots, concordance, Seifert surface, signature, slice knot, slice genus.

do not always exist, and when they do, the S -equivalence class of the associated Seifert matrices is not independent of the choice of Seifert surface. This failure helps to explain why there is no satisfactory definition of knot signature for virtual knots.

For higher dimensional knots, the knot signature is the primary tool for understanding concordance, and for classical knots, it is critical to the study of algebraic, topological, and smooth concordance. Our understanding of virtual knot concordance is far from complete, and the knot signature is one of the missing pieces of the puzzle. Extending the knot signature to virtual knots would have immediate implications to several open questions, such as the conjecture in [DKK17] which asserts that for a classical knot K , its virtual slice genus $g_s(K)$ equals its classical 4-ball genus $g_4(K)$. The main result in [BN17] provides partial support for this conjecture by showing that a classical knot is virtually slice if and only if it is classically slice.

In this article, we extend the knot signature to virtual knots by first defining it for a subset of virtual knots called almost classical knots, and then using parity projection to extend it to all virtual knots. A key result in this direction is Theorem 2.9, which shows that if K_0 and K_1 are virtual knots and are concordant, then so are the virtual knots $P_n(K_0)$ and $P_n(K_1)$ obtained under parity projection. Here P_n denotes projection with respect to the mod n Gaussian parity. The signature gives a lower bound on the slice genus, and it applies to show that any classical knot K with $2g_4(K) = |\sigma(K)|$ has virtual slice genus equal its classical 4-ball genus, as conjectured by Dye, Kaestner, and Kauffman in [DKK17].

Before giving more details, we take a moment to review the relevant papers [ILL10] by Im, Lee, and Lee and [CT07] by Cimasoni and Turaev. In [ILL10], Im, Lee, and Lee introduce signature-type invariants, denoted $\sigma_\xi(K)$, for checkerboard colorable virtual knots. The invariants are defined in terms of Goeritz matrices associated to a checkerboard coloring ξ of K , and in general they depend on ξ . It is not clear (and in fact not generally true) that the resulting invariants are invariant under virtual knot concordance. Indeed, in [BCG17a] we present numerous examples of virtual knots which are slice but have $\sigma_\xi(K) \neq 0$. The approach we develop here will allow us to determine under what conditions the invariants $\sigma_\xi(K)$ are concordance invariants, and it provides a framework for deforming the invariants $\sigma_\xi(K)$ using ω -signatures. Even when $\sigma_\xi(K)$ is not a concordance invariant, it can be replaced by a suitable deformation that is invariant under virtual knot concordance.

In [CT07], Cimasoni and Turaev extend many invariants of classical knots, including signatures, to knots in quasi-cylinders. Their results do not immediately give concordance invariants for virtual knots for several reasons. One is that their notion of concordance is more restrictive and does not take into account stable equivalence. Another more serious issue is their assumption that $H_2(M) = 0$ for the quasi-cylinder M . This assumption is key to showing that invariants of S -equivalence classes of Seifert triples give well-defined invariants of knots in quasi-cylinders. However, this condition is not satisfied for a knot K in a thickened surface $\Sigma \times I$, and in that case the S -equivalence class of the Seifert triple is not independent of the choice of Seifert surface. Indeed, in [CT07, §8.4, p. 558] they write “it is very unlikely that any Seifert type invariant can be constructed in this general setting.” They introduce the notion of φ -equivalence to deal with this issue but note that the signatures defined in [CT07, §6] are not invariant under φ -equivalence.

In this paper, we develop an entirely different approach to extending the knot signatures to virtual knots. A virtual knot is called *almost classical* if it can be represented as a homologically trivial knot K in a thickened surface $\Sigma \times I$. Thus, such a knot K bounds a Seifert surface F , which can be used to define Seifert forms. Seifert matrices V^+ and

V^- are given by choosing a basis for $H_1(F)$ and computing the (relative) linking pairing of the positive and negative push-offs of the basis elements. In the case of a classical knot, viewed as a knot K in $S^2 \times I$, it is not difficult to see that V^+ and V^- are transposes of one another and that any two Seifert matrices for K are S -equivalent. Neither of those statements is true in the more general setting of knots in thickened surfaces of higher genus. Thus, one can use the symmetrization of either V^+ or V^- to define signatures $\sigma^+(K, F)$ and $\sigma^-(K, F)$, and we prove that $V^+ + (V^+)^T = V^- + (V^-)^T$ for any (K, F) , thus it follows that $\sigma^+(K, F) = \sigma^-(K, F)$.

For classical knots, the signature of the symmetrized Seifert matrix $V + V^T$ is unchanged under S -equivalence, and this shows that the signature is independent of the choice of Seifert surface. As previously mentioned, if K is an almost classical knot, the S -equivalence class of its Seifert matrices is not a well-defined invariant of K . Consequently, the resulting signatures typically depend on the choice of Seifert surface. This defect is a departure from the situation for classical knots, but as we shall see, it is often useful in obstructing sliceness to be able to consider different Seifert surfaces (see Subsection 4.1).

In any case, we also define the directed Alexander polynomials $\nabla_{K,F}^\pm(t)$ and ω -signatures $\widehat{\sigma}_\omega(K, F)$ for almost classical knots, both of which depend on the choice of Seifert surface F . The two main results here are Theorem 3.6 and 3.7. The first result shows that slice genus $g_s(K)$ is bounded below by $|\widehat{\sigma}_\omega(K, F)|/2$. The second result shows that if K is slice, then there exist polynomials $f^\pm(t) \in \mathbb{Z}[t]$ such that $\nabla_{K,F}^\pm(t) = f^\pm(t)f^\pm(t^{-1})$. This result is the analogue of the Fox-Milnor condition for almost classical knots. We apply these invariants to the problem of determining sliceness and the slice genus of almost classical knots up to six crossings, and the results are summarized in Table 2.

Analogous results for long knots are developed, including the definitions of S -equivalence and algebraic sliceness for almost classical long knots. Furthermore, the Gordon-Litherland pairing is extended to the virtual setting and used to relate the knot signatures defined here to the invariants of [ILL10].

We now give a brief outline of the contents of this paper. In Section 1, we introduce the basic notions such as Gauss diagrams, virtual knot concordance, Carter surfaces, the virtual knot concordance group, and almost classical knots. In Section 2, we review parity and relate parity projection to lifting knots along covers. The main theorem is Theorem 2.9, showing that parity projection preserves concordance. In Section 3, we introduce various invariants for almost classical knots, including the Alexander-Conway polynomials, the knot signature and nullity, and the directed Alexander polynomials and ω -signatures. The main results are Theorems 3.6 and 3.7. In Section 4, we show how to compute the signatures, ω -signatures, and directed Alexander polynomials for almost classical knots. Included is a skein relation for $\nabla_{K,F}^\pm(t)$ (see equation (7)) and a method for computing the signature under a crossing change (see equations (5) and (6)). These computations are applied to the problem of determining the slice genus of almost classical knots up to six crossings, which are given in Table 2. In Section 5, we study long knots. We define S -equivalence and algebraic concordance for almost classical long knots, and we show that the main results continue to hold. In Section 6, we relate the knot signatures to the invariants defined by Im, Lee, and Lee [ILL10]. In Section 7, we present tables of almost classical knots up to six crossings along with their Alexander-Conway polynomials (Table 1), and their graded genus, signatures, ω -signatures, and slice genus (Table 2). Table 3 presents the Seifert pairs for almost classical knots up to six crossings. Figure 17 on p. 34 shows all slice almost

classical knots up to six crossings, and Figure 18 on p. 37 shows almost classical knots up to six crossings realized as knots in thickened surfaces.

Notation: Throughout this paper all homology groups will be taken with \mathbb{Z} coefficients unless otherwise noted. Here we work mainly with smooth concordance, though occasionally the weaker hypothesis of local flatness is sufficient for our purposes. Decimal numbers such as 4.99 and 5.2012 refer to virtual knots in Green's tabulation [Gre04].

1. PRELIMINARIES

Concordance is an equivalence relation on classical knots that was extended to virtual knots in [CKS02, Tur08, Kau15]. Following the latter two approaches, we define virtual knots and links as equivalence classes of Gauss diagrams, which we take a moment to explain.

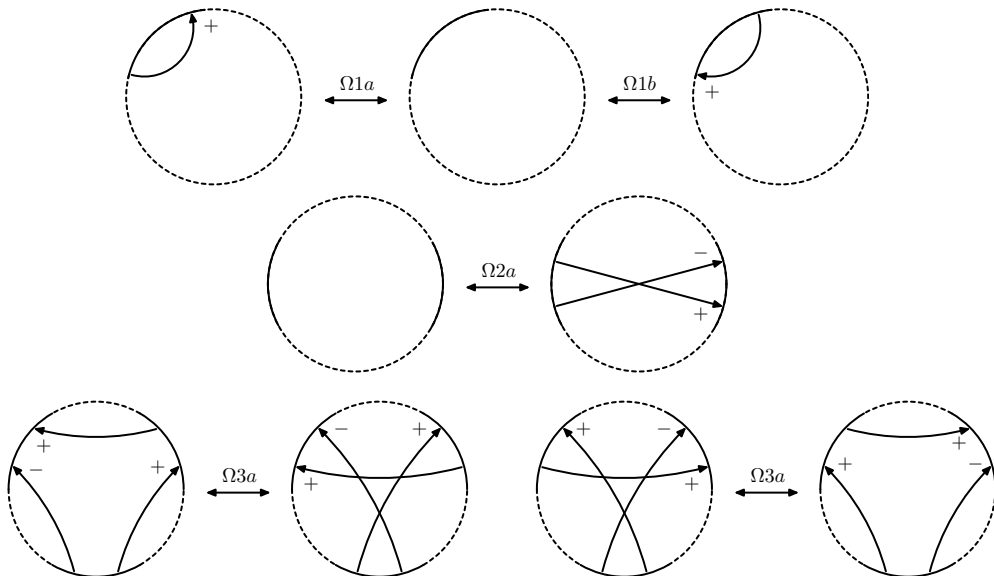


FIGURE 1. Reidemeister moves for Gauss diagrams.

1.1. Gauss diagrams. A Gauss diagram is a decorated trivalent graph consisting of one or more core circles, oriented counterclockwise, together with a finite collection of signed, directed chords, called *arrows*, connecting distinct pairs of points on the circles. Each core circle represents a knotted curve on a surface, and the directed chords connect preimages of the double points of the underlying immersed curve; they point from the over-crossing arc to the under-crossing arc, and their sign (+ or -) indicates the writhe of the crossing. A virtual knot or link is then an equivalence class of Gauss diagrams under the equivalence generated by the Reidemeister moves. In [Pol10], Polyak showed that all Reidemeister moves can be generated by the four moves $\Omega 1a$, $\Omega 1b$, $\Omega 2a$, and $\Omega 3a$, which are depicted for diagrams on one component in Figure 1.

An equivalent and alternative definition for virtual knots and links is as equivalence classes of virtual knot and link diagrams as explained in [Kau99]. Note that a virtual link diagram is said to be oriented if every component has an orientation. We use $-K$ to denote the knot or link with its orientation reversed.

1.2. Virtual knot concordance. We say that two virtual knots K_0 and K_1 are *concordant* if K_0 can be transformed into K_1 by a finite sequence of b births, d deaths, s saddle moves, and Reidemeister moves, such that $s = b + d$. Births, deaths, and saddles are local moves to a virtual knot or link diagram; they are the same as in classical concordance. However, there is an equivalent description of them in terms of Gauss diagrams that is particularly convenient, and these are depicted in Figure 2. Thus a saddle is an oriented smoothing along a chord whose endpoints are disjoint from the endpoints of all other chords, whereas birth and deaths are the addition and removal of a disjoint unknotted component. Saddles are indicated with a dotted line segment as in Figure 2.

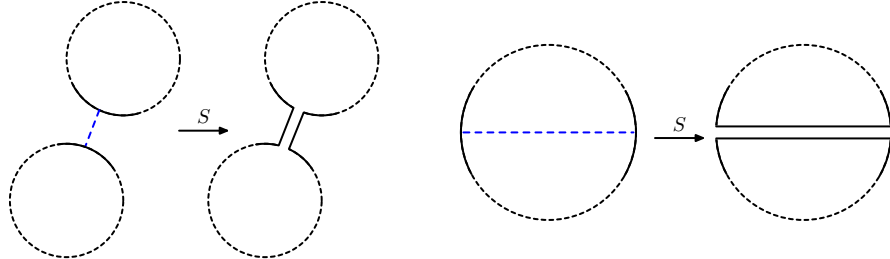


FIGURE 2. Concordance is generated by saddle moves, births and deaths.

Given an arbitrary virtual knot K , it is elementary to show that there exists a finite sequence of births, deaths, and saddles transforming K to the unknot. Given such a sequence, set $g = (s - b - d)/2$, the genus of the surface cobordism from K to the unknot, where b, d, s are the numbers of births, deaths, and saddles, respectively. The *slice genus* of K is defined to be the minimum g over all such sequences. The virtual knot K is said to be *slice* if it is concordant to the unknot, and it is called *ribbon* if it is concordant to the unknot by a sequence of moves that includes only saddles and deaths.

It is not known whether every slice virtual knot is ribbon. This is related to Fox's question, which is whether every classical slice knot is ribbon [Fox62]. Note that there could be classical knots which are virtually ribbon but not classically ribbon, i.e., knots which admit ribbon virtual knot diagrams but not ribbon classical knot diagrams. Thus, a weaker version of Fox's question is whether every classical knot that is slice is virtually ribbon.

1.3. Concordance of knots in thickened surfaces. Given a Gauss diagram D , we review the construction of the Carter surface Σ . Our explanation is based on [Car91], and the analogous construction for virtual knot diagrams is in [KK00].

Suppose that D has n chords on the core circle O , which is oriented counterclockwise. The portions of O from one crossing to the next are called arcs. We thicken O to give an annulus and perform n plumbings, one for each chord, according to its sign (see Figure 3). This results in an oriented surface with boundary, and we form a closed surface by gluing disks to each boundary component of the plumbed annulus. The resulting closed oriented surface is called the *Carter surface*.

Conversely, given a knot K in a thickened surface $\Sigma \times I$, its crossing information determines a Gauss diagram which in turn determines a virtual knot. Stabilization of a knot K in a thickened surface $\Sigma \times I$ is the result of performing surgery on Σ by attaching a 1-handle disjoint from K . The opposite procedure is called *destabilization*, and it involves surgery on Σ removing a 1-handle disjoint from K . Notice that stabilization and destabilization do not affect the underlying Gauss diagram, so they preserve the associated virtual knot. Two

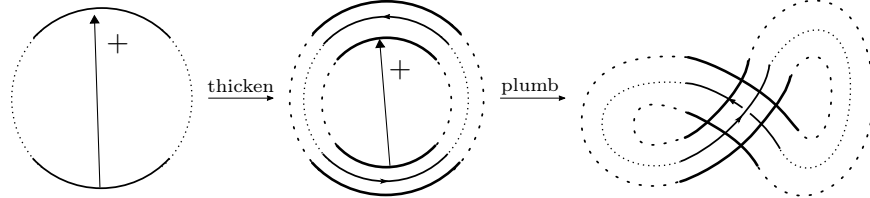


FIGURE 3. Plumbing along a chord in a Gauss diagram.

knots K_0 in $\Sigma_0 \times I$ and K_1 in $\Sigma_1 \times I$ in thickened surfaces are *stably equivalent* if they become equivalent under a finite number of stabilizations and destabilizations. By results of [CKS02], there is a one-to-one correspondence between virtual knots and knots in thickened surfaces up to stable equivalence.

In [Tur08], Turaev studied concordance for knots in thickened surfaces, which he defined as follows.

Definition 1.1. Two oriented knots K_0 in $\Sigma_0 \times I$ and K_1 in $\Sigma_1 \times I$ are called *concordant* if there exists an oriented 3-manifold M with $\partial M \cong -\Sigma_0 \sqcup \Sigma_1$ and an annulus $A \subset M \times I$ with $\partial A = -K_0 \sqcup K_1$. A knot K in $\Sigma \times I$ which is concordant to the unknot is called *slice*.

One can verify that stably equivalent knots are concordant, and thus concordance of knots in surfaces induces an equivalence relation on virtual knots. By [CKS02, Lemma 12], it follows that this notion of concordance for virtual knots is equivalent to the previous definitions given above.

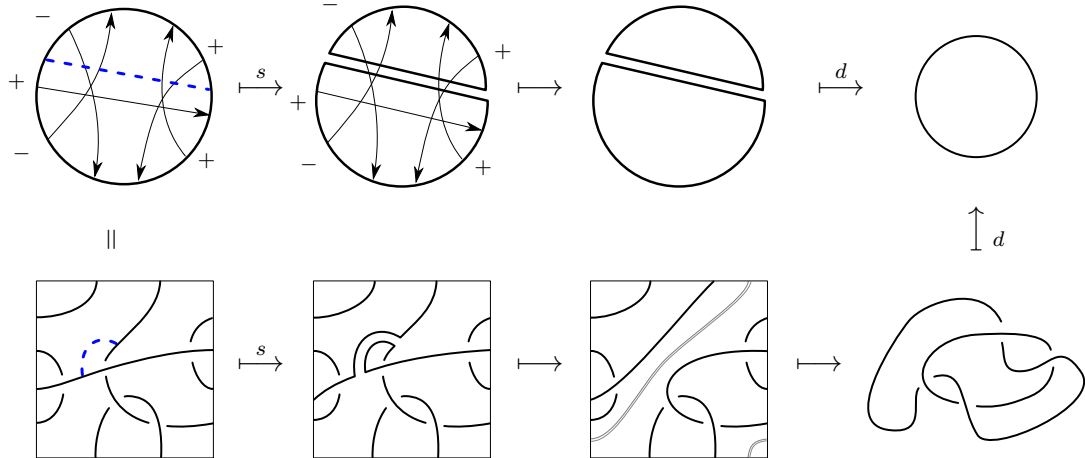


FIGURE 4. A side-by-side comparison of virtual knot cobordism, and cobordism of the knot in the surface. The torus is destabilized along the grey curve to obtain the bottom right diagram.

1.4. The concordance group of long virtual knots. A long virtual knot is defined as an equivalence class of long Gauss diagrams under the Reidemeister moves. A long Gauss diagram is a decorated trivalent graph consisting of one horizontal line oriented from left to right together with a finite collection of signed arrows connecting distinct pairs of points

on the line. As before, the directed chords point from over-crossing to under-crossing, and their sign indicates the local writhe of the crossing.

Alternatively, long virtual knots can be defined as equivalence classes of long virtual knot diagrams see for instance [GPV00]. A long virtual knot diagram is a regular immersion of \mathbb{R} into \mathbb{R}^2 which coincides with the x -axis outside of a compact set and has two types of double points: classical and virtual crossings. Classical crossings are drawn to indicate over and under-crossing arcs, and virtual crossings are encircled. Equivalence of virtual knot diagrams is generated by compactly supported planar isotopies together with the generalised Reidemeister moves.

The connected sum $K_1 \# K_2$ of two long virtual knot diagrams is given by concatenating, placing K_1 on the left and K_2 on the right. In general, connected sum is not a commutative operation. Under connected sum, the set of long virtual knots forms a monoid with identity given by the long unknot with its empty diagram representative.

Just as with round virtual knots, we define concordance for long virtual knots by saying that K_0 and K_1 are *concordant* if K_0 can be transformed into K_1 by a finite sequence of b births, d deaths, s saddle moves, and Reidemeister moves, such that $s = b + d$. Under connected sum, the set of concordance classes of long virtual knots forms a group which is denoted \mathcal{VC} (see [Chr17]). Given a long virtual knot K , we use $[K]$ to denote its concordance class, which is an element of \mathcal{VC} . Note that a long virtual knot K is slice if and only if $[K]$ represents the identity element in \mathcal{VC} . The concordance inverse K^{-1} is the knot obtained by changing the signs of all the arrows and reversing the orientation of K , see Figure 5.

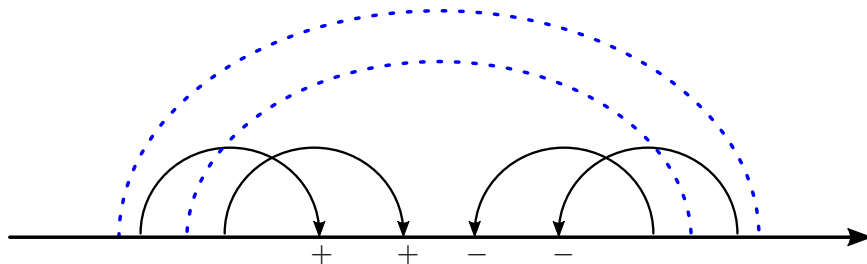


FIGURE 5. The connected sum of a long virtual knot and its inverse is slice.

By the main result of [BN17], the natural inclusion from classical knots to long virtual knots gives an injective homomorphism $\mathcal{C} \rightarrow \mathcal{VC}$, where \mathcal{C} denotes the classical knot concordance group.

1.5. Almost classical knots. In this subsection, we give three equivalent definitions of the index of a crossing c in a virtual knot K in terms of its three representations, namely as a virtual knot diagram, as a Gauss diagram, and as a knot diagram on a surface.

We begin with a review of *virtual linking numbers*. Suppose $L = J \cup K$ is a virtual link with two components, and define $v\ell k(J, K)$ as the sum of the writhe of the crossings where J goes over K . Notice that if L is classical, then $v\ell k(J, K) = v\ell k(K, J)$, but the virtual Hopf link in Figure 6 shows that this is not true in general.

First, suppose K is a virtual knot diagram and c is a crossing of K . Then the oriented smoothing of K at c is a virtual link diagram with two components K' and K'' , where K' denotes the component that contains the outward pointing over-crossing arc at c . The index of c is defined by setting

$$\text{ind}(c) = v\ell k(K', K'') - v\ell k(K'', K').$$

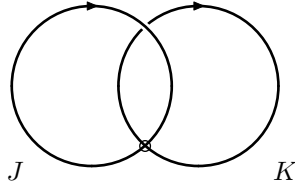


FIGURE 6. The virtual Hopf link has $v\ell k(J, K) = 1$ and $v\ell k(K, J) = 0$

Now suppose c is an arrow in a Gauss diagram D , which we draw with c pointing up. Set

$$\text{ind}(c) = r_+(c) - r_-(c) + \ell_-(c) - \ell_+(c),$$

where $r_{\pm}(c)$ are the numbers of \pm -arrows intersection c and pointing to the right, and $\ell_{\pm}(c)$ are the numbers of \pm -arrows pointing to the left. An easy exercise shows that $v\ell k(K', K'') = r_+(c) - r_-(c)$ and $v\ell k(K'', K') = \ell_+(c) - \ell_-(c)$, thus this definition of $\text{ind}(c)$ agrees with the previous one.

Lastly, suppose $K \subset \Sigma \times I$ is a knot in a thickened surface, and let $p: \Sigma \times I \rightarrow \Sigma$ denote the projection map. For any crossing c of K , let K' and K'' be the two components obtained from the oriented smoothing at c as above and set

$$(1) \quad \text{ind}(c) = [p_*(K')] \cdot [p_*(K'')],$$

the algebraic intersection of the homology classes $[p_*(K')], [p_*(K'')] \in H_1(\Sigma)$.

Given a classical knot K represented as a knot in $S^2 \times I$, then the Jordan curve theorem implies that every chord c of K has $\text{ind}(c) = 0$. The converse is however false, and virtual knots such that each chord has index zero are called *almost classical* [SW06].

Definition 1.2. A virtual knot K is *almost classical* if it can be represented by a Gauss diagram D such that every chord c satisfies $\text{ind}(c) = 0$.

One can alternatively define almost classical knots as those admitting Alexander numberable diagrams, and this approach generalizes to define almost classical links. As explained in [BGH⁺17], a virtual link is almost classical if and only if it can be represented by a homologically trivial link in a thickened surface.

The notion of index extends to long virtual knot diagrams, and a long virtual knot is called *almost classical* if it admits a long Gauss diagram such that every chord has index zero. Equivalently, a long virtual knot diagram is almost classical whenever its closure is almost classical as a virtual knot diagram. We will return to these considerations in Section 5.

2. PARITY, PROJECTION, AND CONCORDANCE

The main result in this section is that parity projection preserves concordance. We derive this result by interpreting parity projection in terms of lifting knots to coverings. We begin by introducing parity and projection.

2.1. Parity and projection. A parity is a collection of functions $\{f_D\}$, one for each Gauss diagram D in the *diagram category*, which is a category \mathcal{D} whose objects are Gauss diagrams and whose morphisms are compositions of Reidemeister moves. Given $D \in \text{ob}(\mathcal{D})$, the function f_D is a map from the chords of D to the set $\{0, 1\}$. Chords c with $f_D(c) = 1$ are called *odd*, and those with $f_D(c) = 0$ are called *even*. The collection $\{f_D \mid D \in \text{ob}(\mathcal{D})\}$ of functions is required to satisfy the following:

Parity axioms. Suppose D and D' are related by a single Reidemeister move.

- (0) The parity of chords not participating in the Reidemeister move does not change.
- (1) If D and D' are related by a Reidemeister I move which eliminates the chord c_0 of D , then, $f_D(c_0) = 0$.
- (2) If D and D' are related by a Reidemeister II move which eliminates the chords c_1 and c_2 of D , then, $f_D(c_1) = f_D(c_2)$.
- (3) If D and D' are related by a Reidemeister III move, then the parities of the three chords involved in the Reidemeister III move do not change. Moreover, the three parities involved in the move are either all even, all odd, or exactly two are odd.

In [Man10], this is referred to as “parity in the weak sense”. Readers interested in more details on parity are referred to the paper by Nikonov [Nik13].

Given a parity f , there is a map on Gauss diagrams called *parity projection* and denoted P_f . For a Gauss diagram D , its image $P_f(D)$ under parity projection is the Gauss diagram obtained from D by eliminating all of its odd chords.

Proposition 2.1 ([Man10]). *If D and D' are two Gauss diagrams equivalent through Reidemeister moves, then their parity projections $P_f(D)$ and $P_f(D')$ are also equivalent through Reidemeister moves.*

This result is a direct consequence of the parity axioms. Although parity projection is defined in terms of the underlying Gauss diagram, Proposition 2.1 implies that it is well-defined as a map on virtual knots.

Since each application of parity projection P_f removes chords from the Gauss diagram D , we have $P_f^{k+1}(D) = P_f^k(D)$ for k sufficiently large. Using this observation, we define $P_f^\infty(D) = \lim_{k \rightarrow \infty} P_f^k(D)$ and we call P_f^∞ the *stable projection* with respect to the parity f . Although stable projection is defined on the level of the Gauss diagrams, it gives rise to a well-defined map on virtual knots.

2.2. Gaussian parity. We mainly consider Gaussian parities, which are defined in terms of the indices of the chords in a Gauss diagram.

Definition 2.2. Let $n > 1$ be an integer and D a Gauss diagram. The *mod n Gaussian parity* is defined by setting, for any chord c of D ,

$$f_n(c) = \begin{cases} 0 & \text{if } \text{ind}(c) = 0 \pmod{n}, \text{ and} \\ 1 & \text{otherwise.} \end{cases}$$

Throughout this paper, we denote mod n Gaussian parity by f_n , its associated parity projection by P_n , and stable projection with respect to f_n by P_n^∞ . For example, the mod n parity projection P_n acts on a Gauss diagram D by removing all chords whose index is nonzero modulo n , and the image of P_n^∞ consists of all Gauss diagrams D with $\text{ind}(c) = 0 \pmod{n}$ for every chord c of D . These virtual knots were studied in [BGH⁺17], where they are called mod n Alexander numberable knots. For instance, a virtual knot is mod n Alexander numberable if and only if it can be represented as a knot K in a thickened surface $\Sigma \times I$ which is homologically trivial in $H_1(\Sigma, \mathbb{Z}/n)$ (see §5 of [BGH⁺17]).

When $n = 2$, one can further show that a virtual knot lies in the image of P_2^∞ if and only if it can be represented by a checkerboard colorable knot.

Another very useful parity is the total Gaussian parity, which is defined next.

Definition 2.3. The *total Gaussian parity* f_0 is defined by setting, for any chord c of D ,

$$f_0(c) = \begin{cases} 0 & \text{if } \text{ind}(c) = 0, \text{ and} \\ 1 & \text{otherwise.} \end{cases}$$

Alternatively, if D is a Gauss diagram, one can define the total Gaussian parity by setting $f_0(c) = \lim_{n \rightarrow \infty} f_n(c)$. Indeed, taking n to be larger than the number of chords of D , one can easily see that $f_n(c) = 0$ if and only if $\text{ind}(c) = 0$.

Throughout this paper, we denote total Gaussian parity by f_0 , its associated parity projection by P_0 , and the stable projection with respect to f by P_0^∞ . For example, the parity projection P_0 acts on a Gauss diagram D by removing all chords whose index is nonzero, and the image of P_0^∞ consists of Gauss diagrams D with $\text{ind}(c) = 0$ for every chord c of D , i.e., almost classical knots.

2.3. Coverings and Parity. In this subsection, we show how to interpret Gaussian parity projection of a virtual knot K represented as a knot in a thickened surface in terms of Turaev's *lifting* along an abelian covering of the surface [Tur08]. Using this approach, we prove that if two virtual knots K_0 and K_1 are concordant, then their images $P_n(K_0)$ and $P_n(K_1)$ under parity projection are concordant (see Theorems 2.9 and 2.11).

In general, if $\pi: \tilde{\Sigma} \rightarrow \Sigma$ is a covering of surfaces and K is a knot in $\Sigma \times I$, then Turaev observed that one can lift K by taking \tilde{K} to be the knot in $\tilde{\Sigma} \times I$ given as a connected component of the preimage $\pi^{-1}(K)$. The equivalence class of \tilde{K} can be shown to be independent of the choice of connected component, and one can define invariants of K in terms of invariants of the lifted knot \tilde{K} .

We review this construction and relate the knots obtained by lifting along abelian covers to those obtained by projection with respect to Gaussian parity. This correspondence gives a natural topological interpretation of parity projections, and we use it to prove that parity projection preserves concordance. We begin with a review of Turaev's construction for lifting knot along covers and explain how it is related to parity projection.

Let $n > 1$ be an integer. Let Σ be a connected closed oriented surface and K be a knot in $\Sigma \times I$. Let $[p_*(K)] \in H_1(\Sigma; \mathbb{Z}/n)$ denote the homology class of K and let $\kappa \in H^1(\Sigma; \mathbb{Z}/n)$ denote its Poincaré dual. By the universal coefficient theorem, there is an isomorphism $\Theta: H^1(\Sigma; \mathbb{Z}/n) \rightarrow \text{Hom}_{\mathbb{Z}}(H_1(\Sigma), \mathbb{Z}/n)$. Fix a basepoint $c \in \Sigma$ and define

$$\psi_K: \pi_1(\Sigma, c) \rightarrow \mathbb{Z}/n$$

by setting $\psi_K = \Theta(\kappa) \circ \rho$, where $\rho: \pi_1(\Sigma, c) \rightarrow H_1(\Sigma)$ is the Hurewicz map. The proof of the next result is an elementary exercise in the various cohomology products defining ψ_K .

Lemma 2.4. *For $\alpha \in \pi_1(\Sigma, c)$, $\psi_K(\alpha) = [\alpha] \cdot [K] \pmod{n}$.*

The kernel of ψ_K yields a regular covering space $\Sigma^{(n)} \rightarrow \Sigma$ of finite index. Moreover, the map sends K to 0. Hence, K lifts to a knot $K^{(n)}$ in $\Sigma^{(n)} \times \mathbb{R}$. As any lift $K^{(n)}$ of K may be obtained from any other lift by a diffeomorphism¹ of Σ , all lifts of K represent the same virtual knot. The knot $K^{(n)}$ is called a *lift* of K .

Example 2.5. If the map $\psi_K: \pi_1(\Sigma, c) \rightarrow \mathbb{Z}/n$ is trivial, then $\Sigma^{(n)} = \Sigma$ and $K^{(n)} = K$. If the group of covering transformations of $\Sigma^{(n)} \rightarrow \Sigma$ is non-trivial and at each crossing point of

¹Turaev uses the term *diffeomorphic* to describe this particular equivalence of knots.

K the over-crossing arc and under-crossing arc lift to different sheets, then $K^{(n)}$ is a simple closed curve on $\Sigma^{(n)}$ representing the trivial virtual knot.

The next lemma relates the lift $K^{(n)}$ of a virtual knot K to its image $P_n(K)$ under mod n parity projection.

Lemma 2.6. *Let K be a knot in $\Sigma \times I$ and $K^{(n)}$ the lift of K to the covering space $\Sigma^{(n)} \times I$. Then the Gauss diagram $D^{(n)}$ of $K^{(n)}$ is obtained from the Gauss diagram D of K by deleting the chords c with $\text{ind}(c) \not\equiv 0 \pmod{n}$. In particular, as virtual knots, the lift $K^{(n)}$ of K is equivalent to its image $P_n(K)$ under parity projection.*

Proof. Let $c \in \Sigma$ be a double point of $p_*(K)$, where $p: \Sigma \times I \rightarrow \Sigma$. Applying the oriented smoothing at c gives knots K' and K'' on $\Sigma \times I$, and using equation (1) and the fact that $\alpha \cdot \alpha = 0$ holds for any $\alpha \in H_1(\Sigma)$, we see that

$$\text{ind}(c) = [p_*(K')] \cdot [p_*(K'')] = [p_*(K')] \cdot [p_*(K)].$$

Now viewing $p_*(K')$ as an element of $\pi_1(\Sigma, c)$, the lifting criterion and Lemma 2.4 imply that $p_*(K')$ lifts to a closed curve in the covering space $\Sigma^{(n)}$ precisely when $\text{ind}(c) = [p_*(K')] \cdot [p_*(K)] \equiv 0 \pmod{n}$. On the other hand, if c is a crossing with $\text{ind}(c) \not\equiv 0 \pmod{n}$, then $p_*(K')$ does not lift to a closed curve in the covering space $\Sigma^{(n)} \rightarrow \Sigma$, hence this crossing does not appear in the lifted knot $K^{(n)}$. Thus the Gauss diagram of $K^{(n)}$ is obtained from D by deleting those chords c with $\text{ind}(c) \not\equiv 0 \pmod{n}$. \square

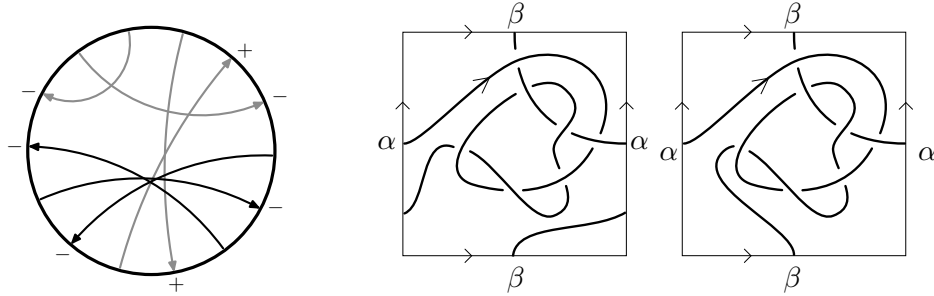


FIGURE 7. A Gauss diagram with two representative knots in $T^2 \times I$.

Example 2.7. Starting with the Gauss diagram D on the left of Figure 7, we find a representative knot in a surface. Its depiction is not unique, as the surface can be stabilized, and Dehn twists can be applied, which alters the homology class represented by the knot diagram. For D , two such representatives are depicted on the right of Figure 7. They are inequivalent as knots in thickened surfaces, but have the same Gauss diagram. Let $K \subset T^2 \times I$ be the knot in the 2-torus depicted on the left in Figure 7, and let $\alpha, \beta \in H_1(T^2)$ be the generators for its first homology. Notice that $[K] = \alpha$, hence, the lift of K to the 2-fold cover is obtained by gluing two copies of T^2 along α and identifying the remaining opposite sides. The lifted knot $K^{(2)}$ is depicted in Figure 8, and one can check that the Gauss diagram $D^{(2)}$ for the lift $K^{(2)}$ is obtained by forgetting the grey arrows of D .

The following lemma, due to Turaev, shows how concordance behaves under lifting knots along coverings.

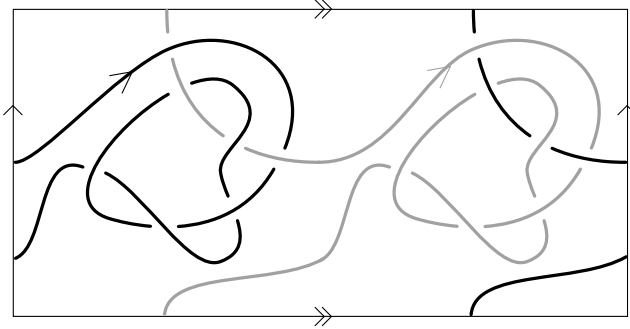


FIGURE 8. Lifting the knot to a two-fold cover

Lemma 2.8 (Lemma 2.1.1, [Tur08]). *If K_0 and K_1 are concordant knots, then the lifted knots $K_0^{(n)}$ and $K_1^{(n)}$ are also concordant.*

The following is the main result in this section, and it implies that parity projection preserves concordance.

Theorem 2.9. *If K_0 and K_1 are virtual knots and K_0 is concordant to K_1 , then their images $P_n(K_0)$ and $P_n(K_1)$ under parity projection are concordant for $n = 0$ and any $n \geq 2$.*

Proof. For $n \geq 2$, the theorem is an immediate consequence of combining Lemmas 2.6 and 2.8. The case $n = 0$ follows from the observation that, for a Gauss diagram with fewer than n chords, $P_0(D) = P_n(D)$. \square

Example 2.10. Consider the virtual knot $K = 6.89907$, whose Gauss diagram appears on the left in Figure 9. In [BCG17b], we show that it has virtual slice genus $g_s(K) \leq 1$. Applying parity projection with respect to total Gaussian parity, the resulting knot $K' = P_0(K)$ has Gauss diagram on the right in Figure 9. We see that K' is the reverse of 4.017, and in [BCG17a] we show that 4.107 has graded genus $\vartheta(K') = 1$. It follows that K' is not slice, and Theorem 2.9 implies that K is also not slice. Hence $g_s(K) = 1$.

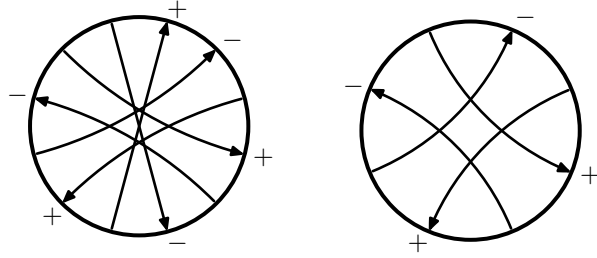


FIGURE 9. Gauss diagrams of 6.89907 and the reverse of 4.107.

The next result follows by repeated application of Theorem 2.9.

Theorem 2.11. *If K_0 and K_1 are virtual knots and K_0 is concordant to K_1 , then their images $P_n^\infty(K_0)$ and $P_n^\infty(K_1)$ under stable projection are concordant for any $n \geq 2$ and $n = 0$.*

In particular, taking $n = 0$ in Theorem 2.11 allows us to reduce questions about concordance of virtual knots to questions about concordance of almost classical knots. We will define signatures for almost classical (long) knots in terms of their Seifert matrices, and Theorem 2.11 shows that such invariants lift to give concordance invariants for all virtual long knots.

Theorem 2.9 says that the projection P_n with respect to Gaussian parity f_n preserves concordance, and it is an interesting question to determine which other parities f have the property that projection P_f preserves concordance.

2.4. Iterated lifts of knots. In this subsection, we present analogues of Lemma 2.6 and Theorem 2.9 for iterated lifts and iterated projections. Given a knot K in the thickened surface $\Sigma \times I$ and a finite sequence of integers n_1, \dots, n_r , with $n_i \geq 2$ for $1 \leq i \leq r$, the iterated lift of K is the knot

$$K^{(n_1, \dots, n_r)} = \left(\dots \left(\left(K^{(n_1)} \right)^{(n_2)} \right) \dots \right)^{(n_r)}$$

in the thickening of the iterated covering space

$$\Sigma^{(n_1, \dots, n_r)} = \left(\dots \left(\left(\Sigma^{(n_1)} \right)^{(n_2)} \right) \dots \right)^{(n_r)}.$$

The next result is obtained by repeated application of Lemma 2.6 and Theorem 2.9.

Proposition 2.12. *Suppose n_1, \dots, n_r are integers with $n_i \geq 2$ for $1 \leq i \leq r$.*

- (i) *As virtual knots, the iterated lift $K^{(n_1, \dots, n_r)}$ of K is equivalent to the image $P_{n_k} \circ \dots \circ P_{n_1}(K)$ under iterated application of parity projection.*
- (ii) *If K_0 and K_1 are virtual knots and K_0 is concordant to K_1 , then their images $P_{n_r} \circ \dots \circ P_{n_1}(K_0)$ and $P_{n_r} \circ \dots \circ P_{n_1}(K_1)$ under iterated projections are concordant.*

Proposition 2.12 raises the question of commutativity of iterated projections, and the simplest instance is whether we have equality of the lifts $K^{(n,m)} = K^{(m,n)}$, or equivalently whether we have equality of the projections $P_m \circ P_n(K) = P_n \circ P_m(K)$? More generally, one can ask to whether the iterated lifts $K^{(n_1, \dots, n_r)}$ are independent of the order n_1, \dots, n_r ? To that end, let $N^{(n_1, \dots, n_r)}$ denote the normal subgroup of $\pi_1(\Sigma, c)$ defining the covering space $\Sigma^{(n_1, \dots, n_r)} \rightarrow \Sigma$. The relationship between the lifts of K is entirely determined by the structure of the lattice of normal subgroups of $\pi_1(\Sigma, c)$. Thus, the question of commutativity of iterated lifts is really a question about the structure of the lattice of normal subgroups.

Consider, for example, the portion of the lattice of regular covering spaces in the commutative diagram below. Here $n, m \geq 2$ are integers, and q is any non-zero multiple of $\text{lcm}(n, m)$. The expression on each arrow corresponds to the index of the covering projection. For simplicity of exposition, we will assume that the indices of the covering maps are as indicated, although this need not be the case in general. Note that since $m|q$ and $n|q$ there are natural maps $\mathbb{Z}/q \rightarrow \mathbb{Z}/n$ and $\mathbb{Z}/q \rightarrow \mathbb{Z}/m$. It follows from the definition of ψ_K that $N^{(q)} \subset N^{(n)} \cap N^{(m)}$. Hence, $\Sigma^{(q)} \rightarrow \Sigma^{(n)}$ and $\Sigma^{(q)} \rightarrow \Sigma^{(m)}$ are also covering projections.

$$\begin{array}{ccccc}
\Sigma^{(n,m)} & & \Sigma^{(q)} & & \Sigma^{(m,n)} \\
\searrow m & \swarrow q/n & \downarrow q & \searrow q/m & \swarrow n \\
\Sigma^{(n)} & & \Sigma^{(m)} & & \Sigma^{(m,n)} \\
\searrow n & & \swarrow m & & \\
& \Sigma & & &
\end{array}$$

Furthermore, the homotopy class of K is an element of each of $N^{(n)}$, $N^{(m)}$, and $N^{(q)}$. Since the diagram commutes, it follows from the lifting criterion that $K^{(q)}$ is a lift of both $K^{(n)}$ and $K^{(m)}$. The following theorem shows how to obtain the Gauss diagram of $K^{(q)}$ from that of either $K^{(n)}$ or $K^{(m)}$. In this instance, it follows that $K^{(n,m)} = K^{(m,n)}$.

Theorem 2.13. *The Gauss diagram $D^{(q)}$ of $K^{(q)}$ is obtained from the Gauss diagram $D^{(m)}$ of $K^{(m)}$ by deleting the chords whose index in K are $\equiv 0 \pmod{m}$ and $\not\equiv 0 \pmod{q}$. Similarly, $D^{(q)}$ is obtained from the Gauss diagram $D^{(n)}$ of $K^{(n)}$.*

Proof. The Gauss diagram $D^{(q)}$ is obtained from D by deleting those chords having index $\not\equiv 0 \pmod{q}$, and $D^{(m)}$ is obtained from D by deleting those chords that have index $\not\equiv 0 \pmod{m}$. Since $m|q$, the only chords of D that need to be deleted from $D^{(m)}$ to obtain $D^{(q)}$ are those having index $\equiv 0 \pmod{m}$ and $\not\equiv 0 \pmod{q}$. \square

On the other hand, by Lemma 2.6, the Gauss diagram $D^{(m,n)}$ can be obtained from $D^{(m)}$ by deleting chords in $D^{(m)}$ with index $\not\equiv 0 \pmod{n}$. We may similarly obtain $D^{(n,m)}$ from $D^{(n)}$. In the general case, it is not always true that $D^{(m,n)} = D^{(n,m)}$, and in certain cases, it may turn out that the iterated covering $\Sigma^{(m,n)} \rightarrow \Sigma$ is nonabelian, as explained in the next proposition.

Proposition 2.14. *The group Γ of covering transformations of $\Sigma^{(m,n)} \rightarrow \Sigma$ is a group extension of \mathbb{Z}/n by \mathbb{Z}/m . In other words, there is short exact sequence*

$$1 \longrightarrow \mathbb{Z}/n \longrightarrow \Gamma \longrightarrow \mathbb{Z}/m \longrightarrow 1.$$

Proof. This follows immediately from the third isomorphism theorem, since

$$\frac{\pi_1(\Sigma, c)}{N^{(m)}} \cong \frac{\pi_1(\Sigma, c)/N^{(m,n)}}{N^{(m)}/N^{(m,n)}}.$$

\square

Example 2.15. Figure 10 shows a Gauss diagram D such that $P_2(P_3(D)) \neq P_3(P_2(D))$. One can easily check that the four diagrams $P_2(D)$, $P_3(D)$, $P_2(P_3(D))$, and $P_3(P_2(D))$ all represent distinct virtual knots. Notice that $P_2(P_3(D)) = P_6(D)$, thus $K^{(3,2)}$ is a knot in the abelian 6-fold cover. On the other hand, $K^{(2,3)}$ is a knot in the non-abelian cover whose associated covering group G is isomorphic to the dihedral group of order 6 and sits in the short exact sequence

$$1 \rightarrow \mathbb{Z}/3 \rightarrow G \rightarrow \mathbb{Z}/2 \rightarrow 1.$$

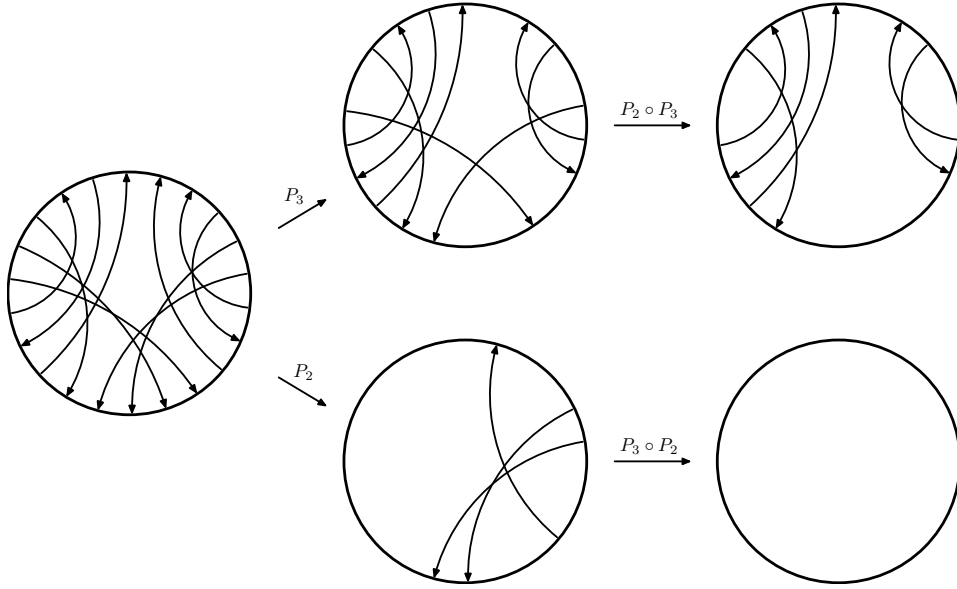


FIGURE 10. In the Gauss diagram above, all chords have negative sign. For the diagram D , notice that $P_2 \circ P_3(D) \neq P_3 \circ P_2(D)$.

2.5. Structure of the virtual knot concordance group. Let \mathcal{VC} denote the group of concordance classes of long virtual knots, and let \mathcal{A} denote the subgroup of \mathcal{VC} generated by almost classical long knots. Because the writhe polynomial $W_K(t)$ vanishes on almost classical knots and is a concordance invariant [BCG17a], this shows that \mathcal{A} is a proper subgroup of \mathcal{VC} . Furthermore, using Turaev's graded genus [Tur08], which is shown to be a concordance invariant of virtual knots in [BCG17a], one can show that the concordance group \mathcal{C} of classical knots is a proper subgroup of \mathcal{A} . In summary, then we have strict inclusions

$$\mathcal{C} \subsetneq \mathcal{A} \subsetneq \mathcal{VC}.$$

By Theorem 2.11, P_0^∞ induces a well-defined surjection $\varphi: \mathcal{VC} \rightarrow \mathcal{A}$. Let $N = \ker(\varphi)$ be the normal subgroup given by the kernel of φ . Thus, we obtain a short exact sequence

$$(2) \quad 1 \rightarrow N \rightarrow \mathcal{VC} \rightarrow \mathcal{A} \rightarrow 1.$$

The inclusion map $\mathcal{A} \hookrightarrow \mathcal{VC}$ gives a splitting of (2), and it follows that

$$(3) \quad \mathcal{VC} = N \rtimes \mathcal{A}$$

is a semidirect product, where the action of \mathcal{A} on N is given by conjugation.

The subgroup N consists of concordance classes of virtual knots whose image $[P_0^\infty(K)]$ is virtually slice. In particular, any virtual knot K containing only chords with nonzero index has its concordance class lying in N . More generally, given a virtual long knot K , the connected sum $K \# (P_0^\infty(K))^{-1}$ lies in N , and every element of N is concordant to a virtual knot of this form.

Turaev's polynomial invariants $u_\pm(K)$ vanish on \mathcal{A} (see [Tur08]) and are concordance invariants, and using them one can conclude that N is infinitely generated.

It is an open problem to determine whether the virtual knot concordance group \mathcal{VC} is abelian. If it were, then the decomposition (3) would be a direct sum. On the other hand,

since the connected sum $K_1 \# K_2$ operation is commutative if either K_1 or K_2 is classical, it follows that the classical concordance group \mathcal{C} lies in the centre of \mathcal{VC} . Thus, we have central extensions

$$\mathcal{C} \rightarrow \mathcal{VC} \rightarrow Q_1 \quad \text{and} \quad \mathcal{C} \rightarrow \mathcal{AC} \rightarrow Q_2$$

for groups Q_1 and Q_2 . It would be interesting to know more about the structure of the quotients Q_1 and Q_2 . For instance, for an almost classical knot K , nontriviality of its graded genus detects that the image of $[K]$ is nontrivial in Q_2 .

Another interesting open problem is to whether the virtual knot concordance group \mathcal{VC} contains elements with finite order which are not concordant to classical knots. It would be especially interesting to find elements with finite order different from two.

3. THE SIGNATURE OF ALMOST CLASSICAL KNOTS

In this section, we recall the Seifert pairing from [BGH⁺17] and use it to define invariants of almost classical knots. We extend the signature and Levine-Tristram signatures to almost classical knots, where unlike in the classical case, they depend on the choice of Seifert surface. Also, we introduce the directed Alexander polynomials of the pair (K, F) , where K is an almost classical knot and F is a Seifert surface. These are two distinct generalizations of the Alexander-Conway polynomial. The main results are Theorems 3.6 and 3.7, which show that the Tristram-Levine signatures provide lower bounds on the slice genus and that the directed Alexander polynomials give slice obstructions.

3.1. Linking numbers. We review the basic properties of the linking numbers in $\Sigma \times I$. Let J, K be disjoint oriented knots in $\Sigma \times I$. By [BGH⁺17, Proposition 7.1], we see that the relative homology group $H_1(\Sigma \times I \setminus J, \Sigma \times \{1\})$ is infinite cyclic and generated by a meridian μ of J . Let $[K]$ denote the homology class of K in $H_1(\Sigma \times I \setminus J, \Sigma \times \{1\})$, and define $\ell k(J, K)$ to be the unique integer m such that $[K] = m\mu$. The linking number $\ell k(J, K)$ can be computed as $J \cdot B$, the algebraic intersection number, where B is a 2-chain in $\Sigma \times I$ with $\partial B = K - v$ for some 1-cycle v in $\Sigma \times \{1\}$. In practice, to compute $\ell k(J, K)$, we count, with sign, the number of times that J crosses above K in $\Sigma \times I$. Here, “above” is taken with respect to the positive I -direction in $\Sigma \times I$. Thus, computing the linking number $\ell k(J, K)$ is formally similar to computing the virtual linking number, which were introduced in Subsection 1.5. Linking numbers in $\Sigma \times I$ are not symmetric but rather satisfy (see §10.2 [CT07]):

$$(4) \quad \ell k(J, K) - \ell k(K, J) = p_*[K] \cdot p_*[J],$$

where \cdot is the algebraic intersection number in Σ of the projections of J and K to Σ .

3.2. Seifert matrices and the Alexander-Conway polynomial. Suppose that K is an almost classical link, realized as a homologically trivial link in $\Sigma \times I$. Suppose further that F is a Seifert surface for K . The Seifert forms $\alpha^\pm: H_1(F) \times H_1(F) \rightarrow \mathbb{Z}$ are defined by $\alpha^\pm(x, y) = \ell k(x^\pm, y)$, where x^\pm denote the \pm “pushoffs” of x into $\Sigma \times I \setminus F$. Given an ordered basis $\{a_1, \dots, a_n\}$ of $H_1(F; \mathbb{Z})$, we use V^\pm to denote the matrix representative of α^\pm , respectively. The pair (V^+, V^-) of matrices is called a Seifert pair for K . The Alexander-Conway polynomial of K is then defined by setting

$$\Delta_K(t) = \det \left(t^{1/2} V^- - t^{-1/2} V^+ \right).$$

A proof that $\Delta_K(t)$ is independent of the choice of Seifert surface can be found in [BGH⁺17], and it follows that $\Delta_K(t) \in \mathbb{Z}[t^{1/2}, t^{-1/2}]$ is well-defined up to multiplication by t^g , where g

is the virtual genus of K . (Here, g is the smallest genus among all surfaces Σ containing a representative for K .) In case K is an almost classical knot, then $\Delta_K(t) \in \mathbb{Z}[t, t^{-1}]$.

For classical links, $V^- = (V^+)^{\tau}$, and this shows that $\Delta_K(t)$ is a *balanced* polynomial, i.e., that it satisfies $\Delta_K(t) = \Delta_K(t^{-1})$. On the other hand, if K is an almost classical knot, it is no longer true that V^- equals $(V^+)^{\tau}$, and so $\Delta_K(t)$ is not necessarily balanced.

3.3. Signature for almost classical knots. Suppose that K is an almost classical link, realized as a link in $\Sigma \times I$, and that F is a Seifert surface for K in $\Sigma \times I$. The *signature* and *nullity* of the pair (K, F) are defined to be

$$\sigma^{\pm}(K, F) = \text{sig}(V^{\pm} + (V^{\pm})^{\tau}) \quad \text{and} \quad n^{\pm}(K, F) = \text{nullity}(V^{\pm} + (V^{\pm})^{\tau})$$

The following lemma implies that $\sigma^+(K, F) = \sigma^-(K, F)$ and $n^+(K, F) = n^-(K, F)$, and henceforth we use $\sigma(K, F)$ and $n(K, F)$ to denote the signature and nullity of (K, F) .

Lemma 3.1. $V^+ + (V^+)^{\tau} = V^- + (V^-)^{\tau}$.

Proof. First note that for two knots J_1, J_2 on F , $\ell k(J_1^{\pm}, J_2) = \ell k(J_1, J_2^{\mp})$. Let $\{a_1, \dots, a_{2g}\}$ be a collection of simple closed curves on F giving a basis for $H_1(F)$. Writing the Seifert matrices with respect to this basis, we see that V^{\pm} has (i, j) entry

$$\begin{aligned} \ell k(a_i^{\pm}, a_j) &= \ell k(a_j, a_i^{\pm}) + p_*[a_i] \cdot p_*[a_j] \\ &= \ell k(a_j^{\mp}, a_i) + p_*[a_i] \cdot p_*[a_j]. \end{aligned}$$

The first term is the (i, j) entry of the transposed matrix $(V^{\mp})^{\tau}$, thus it follows that $V^+ - V^- = (V^-)^{\tau} - (V^+)^{\tau}$, which proves the lemma. \square

As in the classical case, it is useful to generalize the signature to Tristram-Levine signature functions, and in the case of an almost classical knot, we actually get a pair of signature functions. To define the signature functions, it is first necessary to define the *directed Alexander polynomials*, which are given by setting

$$\nabla_{K,F}^{\pm}(t) = \det \left(t^{1/2} V^{\pm} - t^{-1/2} (V^{\pm})^{\tau} \right).$$

Notice that $\nabla_{K,F}^{\pm}(t) \in \mathbb{Z}[t, t^{-1}]$, and they are balanced polynomials, namely they satisfy $\nabla_{K,F}^{\pm}(t) = \nabla_{K,F}^{\pm}(t^{-1})$. We call $\nabla_{K,F}^+(t)$ the *top* Alexander polynomial and $\nabla_{K,F}^-(t)$ the *bottom* Alexander polynomial. Both polynomials depend on the choice of Seifert surface F , and the top and bottom Alexander polynomials are generally distinct from one another and from the Alexander-Conway polynomial. Of course, for classical knots, all three polynomials coincide; i.e., if K is classical then $\Delta_K(t) = \nabla_{K,F}^+(t) = \nabla_{K,F}^-(t)$. In particular, in this case the top and bottom Alexander polynomials are independent of the choice of Seifert surface.

For ω a complex unit number, $\omega \neq 1$, the matrices $(1 - \omega)V^{\pm} + (1 - \bar{\omega})(V^{\pm})^{\tau}$ are Hermitian, and we define the ω -signatures by setting

$$\hat{\sigma}_{\omega}^{\pm}(K, F) = \text{sig}((1 - \omega)V^{\pm} + (1 - \bar{\omega})(V^{\pm})^{\tau}).$$

If the matrix $(1 - \omega)V^{\pm} + (1 - \bar{\omega})(V^{\pm})^{\tau}$ is non-singular, then we will show that $\hat{\sigma}_{\omega}^{\pm}(K, F)$ provides an obstruction to sliceness of K . We will further relate non-singularity of the above Hermitian matrix to the vanishing of $\nabla_{K,F}^{\pm}(\omega)$. As usual, for $\omega = -1$, we have that $\hat{\sigma}_{-1}^{\pm}(K, F) = \sigma(K, F)$. Lemma 3.1 implies that $\nabla_{K,F}^+(-1) = \nabla_{K,F}^-(-1)$, and notice also that $\nabla_{K,F}^{\pm}(-1) \neq 0 \iff n(K, F) = 0$.

3.4. Signatures and concordance. In this subsection, we study the signature functions and the directed Alexander polynomials as obstructions to sliceness. The method of the proof follows that of the classical case (compare with [Lic97]). The main issue is to adapt the classical proof to linking numbers in $\Sigma \times I$, as defined in §3.1.

The main results are Theorems 3.6 and 3.7, and they will follow from a sequence of lemmas, which we now state and prove.

For the next two lemmas, let $K \subset \Sigma \times I$ be a knot in a thickened surface and let W be a compact oriented 3-manifold with $\partial W = \Sigma$. Suppose further that $S \subset W \times I$ is a locally flat surface in $W \times I$ with $K = \partial S$.

Lemma 3.2. *If S is smooth, then the normal bundle of S in $W \times I$ is trivial.*

Proof. Any tubular neighborhood of S is a 2-disk bundle. To show it is trivial, it is sufficient to show its sphere (i.e., $S^1 = U(1)$) bundle is trivial. The classifying map $S \rightarrow BU(1) = \mathbb{CP}^\infty$ determines the bundle up to homotopy. As S is a surface with boundary, it is homotopy equivalent to its 1-skeleton. Since the 1-skeleton of $BU(1)$ is a point, the conclusion follows from the cellular approximation theorem. \square

Lemma 3.3. *The inclusion of pairs $(\Sigma \times I \setminus K, \Sigma \times \{1\}) \hookrightarrow (W \times I \setminus S, W \times \{1\})$ induces an isomorphism in homology $H_1(\Sigma \times I \setminus K, \Sigma \times \{1\}) \rightarrow H_1(W \times I \setminus S, W \times \{1\}) \cong \mathbb{Z}$.*

Proof. By a small homotopy, we may assume S is smooth. Let $i: W \times I \setminus S \rightarrow W \times I$ be inclusion, $p: W \times I \rightarrow W$ be projection onto the first factor, and $j: W \rightarrow W \times I \setminus S$ be defined by $x \rightarrow (x, 1)$. Note that $p \circ i \circ j = \text{id}_W$. Since p_* is an isomorphism, it follows that i_* is a split surjection and j_* is a split injection.

Apply a Mayer-Vietoris argument to $W \times I = (W \times I \setminus S) \cup \text{int}(N(S))$, where $N(S)$ is a closed tubular neighborhood of S in $W \times I$.

$$0 \longrightarrow H_1(U(S)) \longrightarrow H_1(W \times I \setminus S) \oplus H_1(S) \longrightarrow H_1(W \times I) \rightarrow 0.$$

Here $U(S)$ denotes the S^1 -bundle over S obtained by taking the boundary in the fibers of $N(S)$. Also, $N(S) \approx S \times D^2$ because the normal bundle is trivial. Hence, $H_1(U(S)) \cong H_1(S^1) \oplus H_1(S)$. Since j_* is split, the long exact sequence for the pair $(W \times I \setminus S, W \times \{1\})$ splits giving the short exact sequence:

$$0 \longrightarrow H_1(W \times \{1\}) \longrightarrow H_1(W \times I \setminus S) \longrightarrow H_1(W \times I \setminus S, W \times \{1\}) \longrightarrow 0.$$

From the two short exact sequences, we conclude that $H_1(W \times I \setminus S, W \times \{1\})$ is infinite cyclic. Since the summand $H_1(S^1)$ is generated by a meridian of K , we may furthermore conclude that the induced map $H_1(\Sigma \times I \setminus K, \Sigma \times \{1\}) \rightarrow H_1(W \times I \setminus S, W \times \{1\})$ sends a meridian of K to a generator of $H_1(W \times I \setminus S, W \times \{1\})$. Thus the inclusion induces an isomorphism in homology. \square

The next two results are adapted from Lemmas 8.13 and 8.14 in [Lic97]. We provide detailed proofs for completeness.

Lemma 3.4. *For $i = 1, 2$, suppose $\varphi_i: Y_i \rightarrow W \times I$ are maps of orientable surfaces into $W \times I$ such that $\text{im}(\varphi_1) \cap \text{im}(\varphi_2) = \emptyset$ and that $K_i = \varphi_i(\partial Y_i)$ is a knot in $(\partial W) \times I$. Then $\ell k(K_1, K_2) = 0$.*

Proof. Using standard arguments, it may be assumed each φ_1, φ_2 are locally flat embeddings. By definition, $\ell k(K_1, K_2)$ is the homology class of K_2 in $H_1(\Sigma \times I \setminus K_1, \Sigma \times \{1\}) \cong H_1(W \times$

$I \setminus \text{im}(d_1), W \times \{1\}$). Since $\text{im}(\varphi_2) \subset W \times I \setminus \text{im}(\varphi_1)$, K_2 is trivial in $H_1(\Sigma \times I \setminus K_1, \Sigma \times \{1\})$. Thus, $\ell k(K_1, K_2) = 0$. \square

Lemma 3.5. *Let F be a Seifert surface for K in $\Sigma \times I$ and let S be an orientable surface in $W \times I$ with $\partial S = K$. Then there is a two-sided 3-manifold M in $W \times I$ such that $\partial M = F \cup S$ and $M \cap (\Sigma \times I) = F$.*

Proof. The goal is to construct a simplicial map of pairs $\psi: (\overline{W \times I \setminus N(S)}, W \times \{1\}) \rightarrow (S^1, \{-1\})$. We set $M := \psi^{-1}(1)$ and, assuming ψ is appropriately defined, we will have $\partial M = F \cup S$. The map ψ is first defined over the pair $(X, \Sigma \times \{1\})$, where $X := \overline{\Sigma \times I \setminus N(K)}$, and then extended over all of $Z := \overline{W \times I \setminus N(S)}$ using a triangulation. Here we will identify F with $F \cap X$. Consider some arbitrary triangulation of the pair $(Z, W \times \{1\})$. Then $\psi: (Z, W \times \{1\}) \rightarrow (S^1, \{-1\})$ may be defined so that it satisfies all of the following properties:

- (1) ψ is defined on $(X, \Sigma \times \{1\})$ so that on a product neighborhood $F \times [-1, 1]$ of F , the map ψ is $(x, t) \rightarrow e^{i\pi t}$. On the exterior of $F \times [-1, 1]$ in X , ψ is defined to be the constant map $-1 \in S^1$. Note $\Sigma \times \{1\}$ is mapped to $-1 \in S^1$.
- (2) ψ maps ∂Z to S^1 so that $\psi^{-1}(1)$ is $F \times 0 \subset F \times [-1, 1]$ together with $S \times \{x_0\}$. Here $x_0 \in S^1$ is some point identified by the isomorphism $\partial N(S) \approx S \times S^1$.
- (3) ψ can be extended to some spanning tree T of the triangulation so that all 0- and 1-simplices lying in $W \times \{1\}$ are mapped to $-1 \in S^1$.
- (4) ψ is next extended over all 1-simplices so that if c is a 1-cycle formed from a 1-simplex and some edges of T , then $\psi_*([c])$ is given by the composition $H_1(Z, W \times \{1\}) \cong H_1(X, \Sigma \times \{1\}) \rightarrow H_1(S^1, \{-1\}) \cong H_1(S^1)$.
- (5) ψ is then extended sequentially over the 2-, 3-, and 4-simplices so that $W \times \{1\}$ is mapped to $-1 \in S^1$.

Under an appropriate triangulation of S^1 , the map $\psi: (Z, W \times \{1\}) \rightarrow (S^1, \{-1\})$ is simplicial and we conclude that $M := \psi^{-1}(1)$ has a product neighborhood $M \times I$ in $W \times I$. \square

The following theorem establishes the slice obstructions and slice genus bounds from the directed Alexander polynomials and the signature functions.

Theorem 3.6. *Let K be an almost classical knot, represented as a knot in the thickened surface $\Sigma \times I$ with Seifert surface F , and suppose W is an oriented 3-manifold with $\partial W = \Sigma$ and S is an orientable surface in $W \times I$ with $\partial S = K$.*

If $\omega \neq 1$ is a unit complex number such that $\nabla_{K,F}^\pm(\omega) \neq 0$, then $|\widehat{\sigma}_\omega^\pm(K, F)| \leq 2 \text{genus}(S)$. Thus if K is slice, then $\widehat{\sigma}_\omega^\pm(K, F) = 0$, and in particular $\sigma(K, F) = 0$.

Proof. Since it is always true that $|\widehat{\sigma}_\omega^\pm(K, F)| \leq 2 \text{genus}(F)$, we can assume that $\text{genus}(S) \leq \text{genus}(F)$. Let M be the 3-manifold given by Lemma 3.5, so M is compact and oriented and $\partial M = F \cup S$ is a closed surface of genus $g+k$, where g is the genus of F and k is the genus of S . By [Lic97, Lemma 8.16], the subspace $U \subset H_1(\partial M; \mathbb{Z})$ consisting of elements that map to zero under inclusion into $H_1(M, \mathbb{Q})$ has $\text{rank}(U) = g+k$. Thus $U \cap H_1(F; \mathbb{Z})$ has rank at least $g-k$, and we can choose an integral basis $[f_1], \dots, [f_{g-k}]$ of $H_1(F; \mathbb{Z})$ such that $[f_1], \dots, [f_{g-k}]$ lie in U and each f_i is a simple closed curve on F .

Let V^\pm be the $2g \times 2g$ Seifert matrix $(\ell k(f_i^\pm, f_j))$. For $i = 1, \dots, g-k$, there are integers n_i such that $n_i[f_i]$ vanishes in $H_1(M, \mathbb{Z})$. It follows that the curve $n_i f_i$ bounds the image of an orientable surface Y_i mapped into M . Pushing the Y_i into $M \times \{\pm 1\}$ gives surfaces Y_i^\pm disjoint from each Y_j . Thus by Lemma 3.4, $\ell k((n_i f_i)^\pm, n_i f_j) = 0$ for $1 \leq i, j \leq g-k$. This implies that there is a $(g-k) \times (g-k)$ block of zeros in the upper left hand corner of V^\pm .

In general, given a quadratic form Q over a field, a subspace consisting of elements x for which $Q(x) = 0$ is called *isotropic*, and the isotropy index of Q is the dimension of a maximal isotropic subspace. If Q is non-singular with rank N and signature σ , then it is well-known that the isotropy index is given by $\min((N + \sigma)/2, (N - \sigma)/2)$, where $(N + \sigma)/2 = n_+$ and $(N - \sigma)/2 = n_-$, the number of positive and negative eigenvalues of Q .

Since $\omega \neq 1$ and $\nabla_{K,F}^\pm(\omega) \neq 0$, the matrix:

$$(1 - \omega)V^\pm + (1 - \bar{\omega})(V^\pm)^\tau = -(1 - \bar{\omega})(\omega V^\pm - (V^\pm)^\tau)$$

is non-singular. Therefore, the quadratic form associated to the Hermitian matrix $(1 - \omega)V^\pm + (1 - \bar{\omega})(V^\pm)^\tau$ is also non-singular. Since the Seifert matrices V^\pm both have a $(g - k) \times (g - k)$ block of zeros, so does the Hermitian matrix. Thus the isotropy index of the quadratic form is at least $g - k$. Let $\sigma = \hat{\sigma}_\omega^\pm(K, F)$ be the signature of this quadratic form. Since it has rank $2g$, we see that $2(g - k) \leq \min(2g + \sigma, 2g - \sigma)$. Using this, one can easily show that $0 \leq |\hat{\sigma}_\omega^\pm(K, F)| \leq 2k$, and this completes the proof of the theorem. \square

Theorem 3.7. *Let K be an almost classical knot, represented as a knot in the thickened surface $\Sigma \times I$ with Seifert surface F . If K is slice, then there are polynomials $f^\pm(t) \in \mathbb{Z}[t]$ such that $\nabla_{K,F}^\pm(t) = f^\pm(t)f^\pm(t^{-1})$.*

Proof. Let D be a slice disk for K . Repeating the previous argument with $S = D$, it follows that there is a $g \times g$ block of zeros in the upper left hand corner of the Seifert matrices V^\pm . Thus, we can write these matrices in block form:

$$V^\pm = \begin{pmatrix} \mathbf{0} & P^\pm \\ Q^\pm & R^\pm \end{pmatrix},$$

where P^\pm, Q^\pm, R^\pm are $g \times g$ integer matrices.

Thus it follows that

$$\begin{aligned} \nabla_{K,F}^\pm(t) &= \det \begin{pmatrix} \mathbf{0} & t^{1/2}P^\pm - t^{-1/2}(Q^\pm)^\tau \\ t^{1/2}Q^\pm - t^{-1/2}(P^\pm)^\tau & t^{1/2}R^\pm - t^{-1/2}(R^\pm)^\tau \end{pmatrix}, \\ &= \det(tP^\pm - (Q^\pm)^\tau) \det(t^{-1}P^\pm - (Q^\pm)^\tau). \end{aligned}$$

Taking $f^\pm(t) = \det(tP^\pm - (Q^\pm)^\tau)$, the conclusion follows. \square

4. APPLICATIONS

In this section, we apply Theorems 3.6 and 3.7 to the problem of determining the slice genus of almost classical knots up to six crossings, and this step relies on computations of the Seifert matrices (see Table 3) and Turaev's graded genus (see [BCG17a, BCG17b]). We show that the directed Alexander polynomials satisfy a skein relation and how the knot signature changes under a crossing change.

4.1. Computations. In this subsection, we explain how to compute the Seifert matrices and signatures for almost classical knots. To start off, we take a homologically trivial knot in a thickened surface and apply Seifert's algorithm to construct a Seifert surface. This method was used to produce the Seifert matrices V^\pm for almost classical knots with up to 6 crossings in Table 3, namely we applied Seifert's algorithm to the knots in surfaces depicted in Figure 18 and computed linking pairings.

In all computations, the top of the Carter surface is facing up, and the orientation of the Seifert surface determines the direction of the positive and negative push-offs. We follow the conventions of [Lic97] and [BGH⁺17] in this aspect, which means that we parameterize

a regular neighborhood $N(F)$ of the Seifert surface as $F \times [-1, 1]$ such that a small oriented meridian of K enters $N(F)$ at $F \times \{-1\}$ and exits at $F \times \{1\}$. Our convention is that meridians are left-handed.

In performing these computations, it is helpful to organize the almost classical knots into families having the same underlying flat knot. Notice that the oriented smoothing of a knot in a thickened surface depends only on the underlying flat knot. Thus the Seifert surfaces of two knots with the same underlying flat knot differ only in the types of half-twisted bands that are attached. For positive crossings, we attach a left-handed half-twisted band, and for negative crossings, we attach a right-handed half-twisted band.

Example 4.1. Consider the almost classical knots 5.2012, 5.2025, 5.2133, and 5.2433, which all have the same underlying flat knot. Each occurs as a knot in a Carter surface of genus two and admits a Seifert surface of genus two. Two of the knots in this family are slice (5.2025 and 5.2133), and we focus on the other two. Notice also that the diagram for 5.2433 has all negative crossings, and that 5.2012 is obtained by changing one of the crossings of 5.2433 to be positive.

The formulas (5) and (6) below determine the effect on the signature of changing a crossing, and together they imply that the signatures of K_+ and K_- are equal if their directed Alexander polynomials at $t = -1$ have the same sign, otherwise $\sigma(K_+, F_+) = \sigma(K_-, F_-) - 2$.

In this family of 5-crossing almost classical knots, 5.2012 is obtained by performing a crossing change to 5.2433, and each of 5.2025 and 5.2133 are obtained by a crossing change to 5.2012. Since all the knots in the family are related by crossing changes, one can use Conway's method to check the computations.

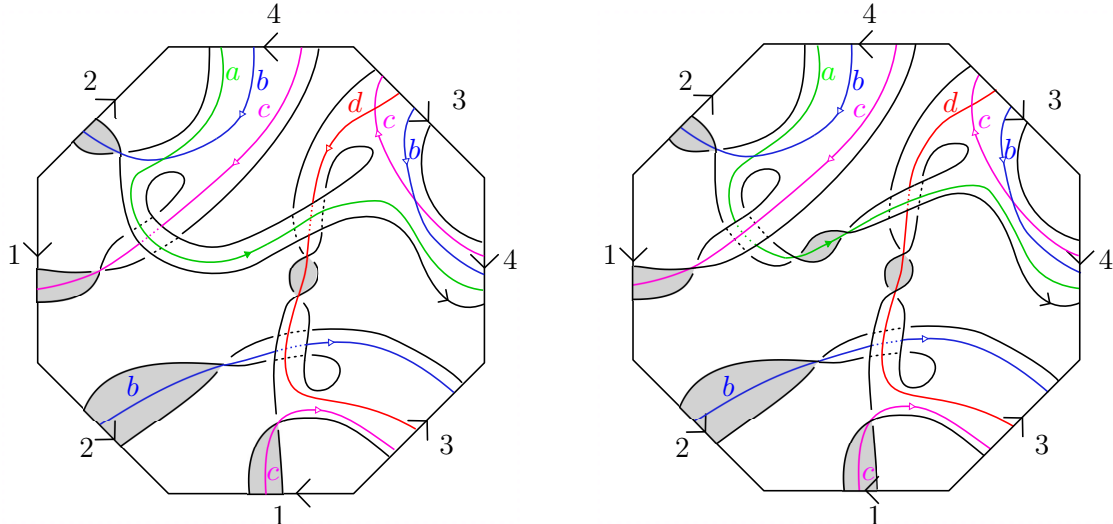


FIGURE 11. Seifert surfaces of the virtual knots 5.2012 (left) and 5.2433 (right).

Consider the Seifert surfaces in Figure 11 for 5.2012 and 5.2433. Also depicted there is a basis $\{a, b, c, d\}$ of simple closed curves for $H_1(F)$. The shaded part of F is the positive side and the unshaded part is the negative side. Thus the positive push-offs of a, b, c, d lie above F along the shaded portion and below it along the unshaded portion. Recall further that if J, K are two simple closed curves in $\Sigma \times I$ that do not intersect, then $\ell k(J, K)$ is an algebraic count of only the crossings when J goes over K (this is because linking is taken in the relative homology of the pair $(\Sigma \times I, \Sigma \times \{1\})$).

For 5.2433, one obtains that

$$V^+ = \begin{pmatrix} 1 & 0 & 0 & 1 \\ 0 & 1 & 0 & 0 \\ 1 & 0 & 1 & 0 \\ 0 & -1 & 0 & 1 \end{pmatrix} \quad \text{and} \quad V^- = \begin{pmatrix} 1 & -1 & 0 & 1 \\ 1 & 1 & 1 & 0 \\ 1 & -1 & 1 & 1 \\ 0 & -1 & -1 & 1 \end{pmatrix}.$$

Thus $\Delta_K(t) = t^2 - 2t + 4 - 3t^{-1} + t^{-2}$ and $\sigma(K, F) = 4$. The directed Alexander polynomials are equal in this case and given by $\nabla_{K,F}^\pm(t) = t^2 - t + 1 - t^{-1} + t^{-2}$. It has roots $e^{\pm 2\pi i/5}, e^{\pm 2\pi i 3/5}$ at the fifth roots of -1 , and $\widehat{\sigma}_\omega^\pm(K, F)$ takes values $\{0, 2, 4\}$.

For 5.2012, one obtains that

$$V^+ = \begin{pmatrix} 0 & 0 & -1 & 1 \\ 0 & 1 & 0 & 0 \\ 0 & 0 & 0 & 0 \\ 0 & -1 & 0 & 1 \end{pmatrix} \quad \text{and} \quad V^- = \begin{pmatrix} 0 & -1 & -1 & 1 \\ 1 & 1 & 1 & 0 \\ 0 & -1 & 0 & 1 \\ 0 & -1 & -1 & 1 \end{pmatrix}.$$

Thus $\Delta_K(t) = t$ and $\sigma(K, F) = 2$. The directed Alexander polynomials are again equal and given by $\nabla_{K,F}^\pm(t) = t - 1 + t^{-1}$. It has roots $e^{\pm 2\pi i/3}$ at the third roots of -1 , and $\sigma_\omega^\pm(K, F)$ takes values $\{0, 2\}$. Notice that $\nabla_{K,F}^\pm(-1) = -3$, which is the opposite sign of what it is in the previous case for 5.2433, and thus (5) and (6) imply that the signature decreases by 2 with the change in crossing in going from 5.2433 to 5.2012., as it does.

It should be noted that the Seifert matrices in Table 3 are computed with just one choice of Seifert surface, and different choices would lead to possibly different signatures, ω -signatures, and directed Alexander polynomials. As we shall see, passing to a second Seifert surface is useful in finding slice obstructions for a given almost classical knot.

4.2. Conway's method. Conway developed methods for computing the Alexander polynomial and signatures of classical knots using crossing changes, and these methods carry over to give skein formulas for the directed Alexander polynomials and the signature of almost classical knots. (The Alexander polynomial $\Delta_K(t)$ of almost classical knots also satisfies a skein relation, see [BGH⁺17, Theorem 7.11] for more details.) We begin by reviewing the situation for classical knots.

Suppose K_+ and K_- are classical knots that are identical except at one crossing, which is positive for K_+ and negative for K_- . Choosing Seifert surfaces for K_+ and K_- that differ only in the half-twisted band at the crossing, and choose a basis for its first homology so the first generator passes through the crossing and all the other generators do not. It follows that the Seifert matrices $V(K_+)$ and $V(K_-)$ are the same except for the $(1, 1)$ entry, in fact, we have

$$V(K_+) = \begin{bmatrix} a & u \\ v & W \end{bmatrix} \quad \text{and} \quad V(K_-) = \begin{bmatrix} a+1 & u \\ v & W \end{bmatrix},$$

where a is the self-linking of the first generator, u and v are row and column vectors, respectively, and W represents the Seifert matrix for the two component link K_0 obtained from the 0-smoothing of K . Arguing as in [Gil82], it follows that the Alexander polynomials satisfy the skein relation

$$\Delta_{K_+}(t) - \Delta_{K_-}(t) = (t^{-1/2} - t^{1/2})\Delta_{K_0}(t),$$

and the knot signatures of K_+ and K_- differ by at most two. In fact, one can further show that

$$(5) \quad \sigma(K_+) \leq \sigma(K_-) \leq \sigma(K_+) + 2,$$

so either $\sigma(K_+) = \sigma(K_-)$ or $\sigma(K_+) + 2 = \sigma(K_-)$.

In general, for any non-singular symmetric real matrix, its signature mod 4 is determined by the sign of its determinant. Applying this observation to the symmetrized Seifert matrix of a knot K , since it is a $2g \times 2g$ matrix with $\det(V + V^\tau) = \Delta_K(-1)$, it follows that

$$(6) \quad \sigma(K) = \begin{cases} 0 \pmod{4} & \text{if } \Delta_K(-1) > 0, \\ 2 \pmod{4} & \text{if } \Delta_K(-1) < 0. \end{cases}$$

Thus one can determine $\sigma(K_+)$ from $\sigma(K_-)$ entirely by comparing the signs of $\Delta_{K_+}(-1)$ and $\Delta_{K_-}(-1)$; if the signs are the same then $\sigma(K_+) = \sigma(K_-)$, otherwise $\sigma(K_+) + 2 = \sigma(K_-)$.

Similar formulas hold for almost classical knots provided one uses compatible Seifert surfaces for K_+ , K_- , and K_0 , which will be denoted F_+ , F_- , and F_0 , respectively and which are assumed to be identical except for the half-twisted bands at the crossing. One must further assume that the symmetrized Seifert matrices for K_+ , K_- , and K_0 are all non-singular, which is automatic for classical knots but which does not always hold for almost classical knots. In that case, for an appropriate choices of generators, the Seifert matrices $V^\pm(K_+)$ and $V^\pm(K_-)$ are given by

$$V^+(K_+) = \begin{bmatrix} a & u \\ v & W^+ \end{bmatrix} \quad \text{and} \quad V^+(K_-) = \begin{bmatrix} a+1 & u \\ v & W^+ \end{bmatrix},$$

$$V^-(K_+) = \begin{bmatrix} a & u' \\ v' & W^- \end{bmatrix} \quad \text{and} \quad V^-(K_-) = \begin{bmatrix} a+1 & u' \\ v' & W^- \end{bmatrix}.$$

It follows that the directed Alexander polynomials satisfy the skein relation

$$(7) \quad \nabla_{K_+, F_+}^\pm(t) - \nabla_{K_-, F_-}^\pm(t) = (t^{-1/2} - t^{1/2}) \nabla_{K_0, F_0}^\pm(t)$$

and that equations (5) and (6) continue to hold, where in the second formula $\Delta_K(-1)$ is replaced by $\nabla_{K, F}^\pm(-1)$. (Notice that Lemma 3.1 implies that $\nabla_{K, F}^+(-1) = \nabla_{K, F}^-(-1)$.)

4.3. Slice obstructions. We explain how to apply the previous results to the question of sliceness of almost classical knots. Combined with the graded genus [BCG17a, BCG17b], the computations are sufficient to determine sliceness for all almost classical knots up to six crossings. These results are presented in Table 2 at the end of the paper, which gives the graded genus, signature, and ω -signatures for these knots. The almost classical knots that are known to be slice are also displayed with their slicings in Figure 17.

All the other knots in the table can be seen to be non-slice, and we explain this now. In the majority of cases, this follows by applying Theorem 3.6, using either the signature or ω -signatures. When the signatures and ω -signatures fail to obstruct sliceness, we apply Theorem 3.7 or the graded genus. For instance, the knots $K_1 = 4.108$ and $K_2 = 6.90172$ are classical, and although their signatures and ω -signatures all vanish, their Alexander-Conway polynomials, which are $\Delta_{K_1}(t) = t - 3 + t^{-1}$ and $\Delta_{K_2}(t) = t^2 - 3t + 5 - 3t^{-1} + t^{-2}$ do not factor as $f(t)f(t^{-1})$, and so Theorem 3.7 applies to show that neither K_1 nor K_2 is slice.

In a similar way, one can use the directed Alexander polynomials to obstruct sliceness for the knots 6.87857 and 6.90194. For $K = 6.87857$, the directed Alexander polynomials are $\nabla_{K, F}^+(t) = -2t + 4 - 2t^{-1}$ and $\nabla_{K, F}^-(t) = -t + 6 - t^{-1}$, neither of which factors as $f(t)f(t^{-1})$,

so Theorem 3.7 applies to show it is not slice. Likewise, $K = 6.90194$ has down polynomial $\nabla_{K,F}^-(t) = -t^2 - 3t + 8 - 3t^{-1} + t^{-2}$, which does not factor so K is not slice.

The five almost classical knots 6.77905, 6.77985, 6.78358, 6.85091, and 6.90232 all have graded genus $\vartheta(K) = 1$. Since $\vartheta(K)$ is a concordance invariant of virtual knots [BCG17a], it follows that none of them are slice.

In some cases, we obstruct sliceness using invariants derived from a second Seifert surface F' . The new surface is obtained from the standard one by connecting it to a parallel copy of the Carter surface by a small tube. For instance, for $K = 5.2439$, the new Seifert matrices are

$$V^- = \begin{bmatrix} -1 & 1 & 0 & 0 & 0 & 1 \\ -1 & 0 & 1 & 0 & 1 & 0 \\ 0 & 0 & 1 & 0 & 0 & 0 \\ 0 & 0 & -1 & 1 & 0 & 0 \\ 0 & 0 & 0 & 0 & 0 & 1 \\ 0 & 0 & 0 & 0 & -1 & 0 \end{bmatrix} \quad V^+ = \begin{bmatrix} -1 & 0 & 0 & 0 & 0 & 1 \\ 0 & 0 & 0 & 0 & 1 & 0 \\ 0 & 1 & 1 & -1 & 0 & 0 \\ 0 & 0 & 0 & 1 & 0 & 0 \\ 0 & 0 & 0 & 0 & 0 & 0 \\ 0 & 0 & 0 & 0 & 0 & 0 \end{bmatrix}.$$

From this, it follows that $\sigma(K, F') = 2$, and Theorem 3.6 applies to show K is not slice. For $K = 6.77908$, we find that $\widehat{\sigma}_\omega^\pm(K, F')$ takes values $\{-2, 0\}$, and Theorem 3.6 again shows it is not slice.

In the case of $K = 6.72695$, we have $\nabla_{K,F}^\pm(t) = -t + 3 - t^{-1}$, which does not factor, and Theorem 3.7 applies and gives an obstruction to sliceness. Likewise for $K = 6.87548$, we have $\nabla_{K,F'}^+(t) = -t^2 - t + 5 - t^{-1} - t^{-2}$ and $\nabla_{K,F'}^-(t) = -t + 3 - t^{-1}$, and neither factors, so Theorem 3.7 applies again to show it is not slice.

Table 2 shows, with fewer details, a slice obstruction for each of the remaining non-slice almost classical knots with up to six crossings, and Seifert pairs for all almost classical knots are given in Table 3.

5. LONG KNOTS, S -EQUIVALENCE, AND ALGEBRAIC CONCORDANCE

In this section, we extend the previous results to long virtual knots. In the case of an almost classical long knot, we will show that Seifert pairs are S -equivalent, and it follows that the knot signatures and directed Alexander polynomials are independent of the choice of Seifert surface. We define algebraic sliceness for almost classical long knots and show that any isotropic knot (as defined below) is algebraically slice. We also show that Theorems 3.6 and 3.7 continue to hold provided the underling almost classical long knot is algebraically slice.

5.1. Long knots. The signatures and directed Alexander polynomials for almost classical knots depend on the choice of Seifert surface, which is a departure from how the invariants behave for classical knots. If one instead considers long virtual knots, and more specifically long almost classical knots, one can show that the signatures and directed Alexander polynomials are independent of the choice of Seifert surface. We explain this aspect here.

We define a long virtual knot diagram here to be a round virtual knot diagram with a choice of basepoint $*$, and equivalence is generated by Reidemeister moves that do not interact with the basepoint. A standard argument shows this is equivalent to the definition given in Subsection 1.4. Alternatively, one can represent a long virtual knot as a knot in a thickened surface $\Sigma \times I$ with a basepoint placed on the knot away from the crossings. It is convenient to mark one region of the Carter surface, and we do that by placing a marked point z_0 in the region to the right of the basepoint. The region with the marked point will

be treated as the infinite or “unbounded region,” and the marked point z_0 will play the role of ∞ .

For any crossing c of a long virtual knot K , one can define the index of c in the same way as for round knots. A long knot K is called almost classical if every crossing c of K has $\text{ind}(c) = 0$. Parity and parity projection also extend to the setting of long virtual knots, and it is a routine exercise to establish the analogue of Theorem 2.11 for long knots. We leave the details to the indefatigable reader.

5.2. Seifert surfaces and S -equivalence. Now suppose K is an almost classical long knot, represented as a knot on a thickened surface $\Sigma \times I$ together with a choice of basepoint. Since K is homologically trivial, it admits a Seifert surface F , and here we require that its image $p(F)$ does not contain $\{z_0\}$, where $p: \Sigma \times I \rightarrow \Sigma$ is projection. In other words, we require that the Seifert surface for K lie in $(\Sigma \setminus \{z_0\}) \times I$. To see that this condition can always be satisfied, consider Seifert’s algorithm, as implemented for knots in surfaces. The first step is to smooth all crossings, the second is to find subsurfaces which co-bound the Seifert cycles. At this stage, we choose the subsurface on the side of the cycle opposite to the one containing z_0 . In this way, we ensure that the Seifert surface satisfies $F \subset (\Sigma \setminus \{z_0\}) \times I$.

If F, F' are two Seifert surfaces for K , both lying in $(\Sigma \setminus \{z_0\}) \times I$, then $F \cup (-F')$ is a closed 2-chain that represents the zero element in second homology. (This holds because its image under projection $p: \Sigma \times I \rightarrow \Sigma$ lies in $\Sigma \setminus \{z_0\}$, which has trivial second homology.) This fact implies that any two Seifert surfaces for K lying in $(\Sigma \setminus \{z_0\}) \times I$ are related by surgery, and that implies that the pairs of Seifert matrices from the two surfaces must be S -equivalent. We pause for a moment to define S -equivalence for pairs (V^+, V^-) of Seifert matrices, and we begin by defining row enlargement and reduction, as well as column enlargement and reduction, for Seifert pairs (V^+, V^-) . These operations reflect the change in the Seifert matrices that result from performing surgery on the Seifert surface.

A *Seifert pair* (V^+, V^-) is a pair of integral square matrices satisfying $V^+ + (V^+)^T = V^- + (V^-)^T$ and $\det(V^- - V^+) = 1$. A second Seifert pair (W^+, W^-) is said to be obtained from (V^+, V^-) by *column enlargement* if

$$W^+ = \begin{bmatrix} 0 & 1 & 0 \\ 0 & 0 & u \\ 0 & v & V^+ \end{bmatrix} \quad \text{and} \quad W^- = \begin{bmatrix} 0 & 0 & 0 \\ 1 & 0 & u \\ 0 & v & V^- \end{bmatrix}.$$

Here u is a row vector and v is a column vector. In this case, we also say that (V^+, V^-) is obtained from (W^+, W^-) by *column reduction*. Similarly, a Seifert pair (W^+, W^-) is said to be obtained from (V^+, V^-) by *row enlargement* if

$$W^+ = \begin{bmatrix} 0 & 0 & 0 \\ 1 & 0 & u \\ 0 & v & V^+ \end{bmatrix} \quad \text{and} \quad W^- = \begin{bmatrix} 0 & 1 & 0 \\ 0 & 0 & u \\ 0 & v & V^- \end{bmatrix}.$$

We also say (V^+, V^-) is obtained from (W^+, W^-) by *row reduction*.

Definition 5.1. *S-equivalence* is the equivalence relation on Seifert pairs (V^+, V^-) generated by simultaneous unimodular congruence, row enlargement, row reduction, column enlargement, and column reduction.

One can easily check that, as functions of the Seifert matrices V^\pm , the signature $\sigma(K, F)$, ω -signatures $\widehat{\sigma}_\omega^\pm(K, F)$, and directed Alexander polynomials $\nabla_{K, F}^\pm(t)$ do not change under S -equivalence. Thus, for an almost classical long knot, the signature, ω -signature, and

directed Alexander polynomials are all independent of the choice of Seifert surface. In that case, we write $\sigma(K)$, $\widehat{\sigma}_\omega^\pm(K)$, and $\nabla_K^\pm(t)$ for the signature, ω -signature, and the directed Alexander polynomials of K .

If $\omega \neq 1$ is a unit complex number such that $\nabla_K^\pm(\omega) \neq 0$, then just as with round knots, we see that $\widehat{\sigma}_\omega^\pm(K)$ satisfies the inequality $2g_s(K) \leq |\sigma_\omega^\pm(K)|$ and so gives a lower bound on the slice genus of K . However, in this case, we get the stronger statement that $\widehat{\sigma}_\omega^\pm(K)$ is a concordance invariant of the underlying almost classical long knot K , and the improvement results from the fact that the S -equivalence class of the Seifert pair (V^+, V^-) is independent of choice of Seifert surface, and

$$(1 - \omega)V^\pm + (1 - \bar{\omega})(V^\pm)^\tau = -(1 - \bar{\omega})(\omega V^\pm - (V^\pm)^\tau)$$

is an invariant of the S -equivalence class of the pair (V^+, V^-) .

If K_1 and K_2 are two long almost classical knots and ω is not a root of $\nabla_{K_1 \# K_2}^\pm(t)$, then we have $\sigma_\omega^\pm(K_1 \# K_2) = \sigma_\omega^\pm(K_1) + \sigma_\omega^\pm(K_2)$, which is to say that the ω -signatures define homomorphisms from the monoid of long knots to \mathbb{Z} -valued functions on $S^1 \setminus \{1\}$. In the classical case, this map descends to a homomorphism on the concordance group of classical knots, but that result does not extend to the concordance group of almost classical knots because there are almost classical knots for which $\nabla_K^\pm(\omega) = 0$ for all $\omega \in S^1$ different from 1.

5.3. Algebraic concordance. For almost classical long knots, there is a notion of algebraic concordance, and here we give a brief account. A pair (V^+, V^-) of $2g \times 2g$ matrices is said to be *null-concordant* if they are simultaneously unimodular congruent to matrices in block form:

$$V^\pm = \begin{pmatrix} \mathbf{0} & P^\pm \\ Q^\pm & R^\pm \end{pmatrix},$$

where P^\pm, Q^\pm, R^\pm are integer $g \times g$ matrices. An almost classical long knot K is called *algebraically slice* if it has a pair (V^+, V^-) of Seifert matrices that are null-concordant. The next result is a restatement of Theorems 3.6 and 3.7 for algebraically slice knots.

Theorem 5.2. *Suppose K is an almost classical long knot. If K is algebraically slice and $\omega \neq 1$ is a unit complex number such that $\nabla_K^\pm(\omega) \neq 0$, then $\widehat{\sigma}_\omega^\pm(K) = 0$. Further, there exist polynomials $f^\pm(t) \in \mathbb{Z}[t]$ such that $\nabla_K^\pm(t) = f^\pm(t)f^\pm(t^{-1})$.*

Notice that if an almost classical long knot is slice, then it is algebraically slice.

For classical knots, Kawauchi gives a useful characterization of algebraic sliceness in terms of bounding isotropic surfaces in the 4-ball (see [Kaw96, Theorem 12.2.3]), and we present an analogous result for almost classical knots. We begin with some definitions.

If M is a compact oriented 3-manifold with boundary, then we call a surface $S \subset \partial M$ *isotropic* if $\partial S \approx S^1$ and $\text{rank}(\ker(i_*(H_1(S) \rightarrow H_1(M)))) = \text{genus}(S)$.

Now suppose K is a homologically trivial knot in a thickened surface $\Sigma \times I$ and W is a compact, oriented 3-manifold with $\partial W = \Sigma$. We say that K is *isotropic* if there exist:

- (i) a locally flat, compact, oriented 3-manifold M with boundary in $W \times I$, and
- (ii) compact surface $S \subset \partial M$ whose complement $F = \overline{\partial M \setminus S}$ lies in $\Sigma \times I$ and gives a Seifert surface for K , such that S is isotropic in M .

An almost classical long knot K is called *isotropic* if it can be represented as an isotropic knot in $\Sigma \times I$. The next result implies that isotropic knots are always algebraically slice.

Proposition 5.3. *Suppose K is an almost classical long knot. If K is isotropic, then it is algebraically slice.*

Proof. We represent K as a knot in $\Sigma \times I$ with Seifert surface F and isotropic surface S such that $F \cup S = \partial M$ for a locally flat, compact, oriented 3-manifold M in $W \times I$. (Here, as above, W is a compact oriented 3-manifold with boundary $\partial W = \Sigma$.)

Let $g = \text{genus}(F)$. By [Kaw96, Lemma 12.2.4], we see that F is also isotropic in M . Set $U = \ker(i_*(H_1(F) \rightarrow H_1(M)))$.

Using a collar of M in $W \times I$, it follows that $\ell k(x^\pm, y) = 0$ for all $x, y \in U$. There is a rank g summand of $H_1(F)$ on which the Seifert form vanishes, and this shows that the associated Seifert matrices (V^+, V^-) are null-concordant. It follows that K is algebraically slice. \square

The converse to Proposition 5.3 is true for classical knots, namely a classical knot is isotropic if and only if it is algebraically slice. It is an interesting problem to see whether that result extends to almost classical long knots.

6. THE GORDON-LITHERLAND PAIRING

In this section, we extend the Gordon-Litherland pairing to the setting of almost classical knots and use it to relate the signature defined previously to a signature-type invariant for virtual knots defined in terms of the Goeritz matrix [ILL10]. In [ILL10], the authors used the methods of [GL78] to define invariants of virtual links L that depend on a choice of checkerboard coloring ξ of L .

Checkerboard colorings were first introduced by N. Kamada in [Kam02] in the context of abstract link diagrams, and we give a brief review of the definition. Given a knot or link $K \subset \Sigma \times I$ in a thickened surface, let $p: \Sigma \times I \rightarrow \Sigma$ be projection and set $\bar{K} = p(K)$. Thus \bar{K} is a tetravalent graph on Σ . A *checkerboard coloring* of (Σ, \bar{K}) is a coloring of the components of $\Sigma \setminus \bar{K}$ by two colors, black and white, such that any two components of $\Sigma \setminus \bar{K}$ that share an edge have different colors. Although all classical links admit checkerboard colorings, the same is not true for virtual links. Indeed a virtual link diagram is checkerboard colorable if and only if it can be represented as a link in a thickened surface $\Sigma \times I$ which is null-homologous in $H_1(\Sigma, \mathbb{Z}/2)$ (see p. 966 in [CSW⁺09]).

Given a virtual link diagram D with checkerboard coloring ξ , Im, Lee, and Lee show how to associate a matrix $G_\xi(D)$ called the Goeritz matrix [ILL10]. Neither the matrix nor its signature is a well-defined virtual knot invariant, but modifying the signature of $G_\xi(D)$ with a correction term defined as the sum of the incidence numbers of all type II crossings of D (see Figures 12 and 15), one obtains a number $\sigma_\xi(D) \in \mathbb{Z}$ which depends only on the underlying virtual link and the choice ξ of checkerboard coloring. They also use the Goeritz matrix to define a nullity which we denote $n_\xi(K)$. In case D is a classical diagram, $n_\xi(K) = 0$ and $\sigma_\xi(D)$ is independent of ξ , and in that case it is equal to the knot signature by results of [GL78]. In general, since a virtual link diagram admits at most two inequivalent checkerboard colorings, it follows that the invariants $\sigma_\xi(D), n_\xi(D)$ take on at most two values.

In the previous section, we used the Seifert pairing associated to an almost classical knot K and a Seifert surface F to define its signature $\sigma(K, F)$ and nullity $n(K, F)$. Since every almost classical knot is checkerboard colorable, it is natural to wonder whether the signature $\sigma(K, F)$ and nullity $n(K, F)$ defined here are related to the invariants $\sigma_\xi(K)$ and $n_\xi(K)$ of [ILL10]. In this section, we shall relate these two pairs of invariants. By extending the Gordon-Litherland pairing [GL78] to almost classical knots, we will prove that if K

is an almost classical knot and F is a Seifert surface for K , then $\sigma(K, F) = \sigma_\xi(K)$ and $n(K, F) = n_\xi(K)$ for some checkerboard coloring ξ of K .

To begin, we review the construction of the Goeritz matrix associated to a checkerboard colored virtual knot diagram. For classical knots, this construction was given in [GL78], and it was extended to virtual knots in [ILL10]. Suppose D is a virtual knot diagram on a Carter surface Σ with checkerboard coloring ξ . Let $C_D = \{c_1, \dots, c_k\}$ denote the set of classical crossings of D . We enumerate the white regions X_0, X_1, \dots, X_n of $\Sigma \setminus D$, and for each crossing $c \in C_D$, we define its incidence number $\eta(c) = \pm 1$ with respect to the ξ according to Figure 12.

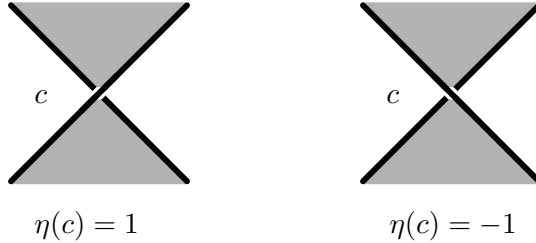


FIGURE 12. The incidence number of a crossing.

Define an $(n + 1) \times (n + 1)$ matrix $G'_\xi(D) = (g_{ij})_{i,j=0,\dots,n}$ by setting

$$g_{ij} = \begin{cases} -\sum \eta(c) & \text{if } i \neq j, \\ -\sum_{k \neq i} g_{ik} & \text{if } i = j. \end{cases}$$

In the above formulas, the first sum is taken over all crossings $c \in C_D$ incident to both X_i and X_j , and the second formula guarantees that $\sum_{j=0}^n g_{ij} = 0$ for each $i = 0, \dots, n$. So the columns of $G'_\xi(D)$ sum to zero.

Definition 6.1. The Goeritz matrix $G_\xi(D)$ is the $n \times n$ matrix obtained by deleting the first row and column from $G'_\xi(D)$. In other words, $G_\xi(D) = (g_{ij})_{i,j=1,\dots,n}$.

Remark 6.2. The Goeritz matrix $G_\xi(D)$ is not an invariant of the knot; it depends on the diagram D , the checkerboard coloring ξ , the order of the white regions, and the choice of X_0 .

Example 6.3. Consider the almost classical knot $K = 4.105$. This knot admits two checkerboard colorings ξ_1 and ξ_2 , and these are depicted in Figure 13. For ξ_1 , there is only one white region X_0 , so $G'_{\xi_1}(D) = [0]$ and $G_{\xi_1}(D)$ is the empty matrix. For ξ_2 , there are three white regions X_0, X_1, X_2 and we compute that

$$G'_{\xi_2}(D) = \begin{bmatrix} -4 & 2 & 2 \\ 2 & -2 & 0 \\ 2 & 0 & -2 \end{bmatrix}, \quad \text{and so} \quad G_{\xi_2}(D) = \begin{bmatrix} -2 & 0 \\ 0 & -2 \end{bmatrix}.$$

We now describe the Gordan-Litherland pairing, extending the methods of [GL78] to the present setting. Suppose D is a virtual knot diagram, Σ is its Carter surface, and ξ a checkerboard coloring of D in Σ . Let F be the spanning surface for D determined by the black regions of the checkerboard coloring and N the closed tubular neighborhood of F in $\Sigma \times I$. (We do not require that spanning surfaces be oriented.) So N is a $[-1, 1]$ -bundle

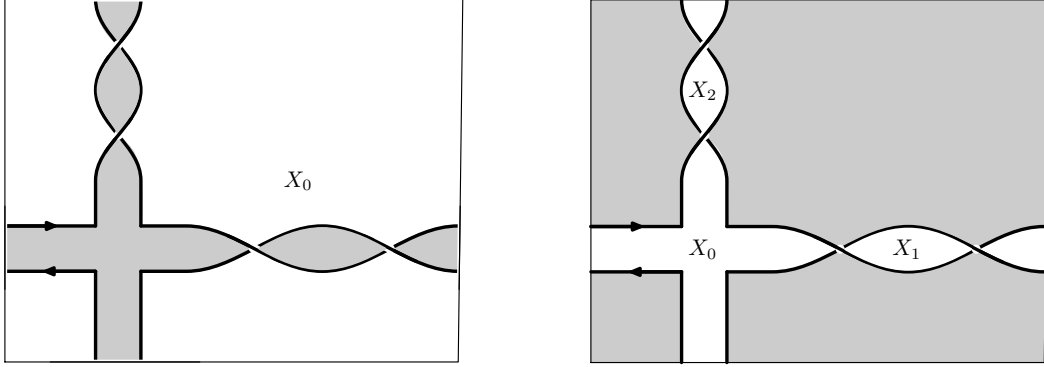


FIGURE 13. Two checkerboard colorings, denoted ξ_1 (left) and ξ_2 (right), for the almost classical knot 4.105.

over F , and we set \tilde{F} to be the associated $\{\pm 1\}$ -bundle, so $\tilde{F} \rightarrow F$ is the orientable double cover when F is not orientable, and it is the trivial double cover otherwise.

Define a pairing $\mathcal{G}_F: H_1(F) \times H_1(F) \rightarrow \mathbb{Z}$ by setting $\mathcal{G}_F(\alpha, \beta) = \ell k(\tau\alpha, \beta)$. Here ℓk refers to the linking number in $\Sigma \times I$ relative to $\Sigma \times \{1\}$, and $\tau: H_1(F) \rightarrow H_1(\tilde{F})$ is the transfer map for the double cover $\tilde{F} \rightarrow F$.

Lemma 6.4. \mathcal{G}_F is symmetric.

Proof. The proof is similar to the one given in [GL78, Prop 9], and we include the argument for completeness. Orient \tilde{F} so that the positive normal vector points out of N , and let $i_{\pm}: \tilde{F} \rightarrow \Sigma \times I \setminus \tilde{F}$ be the positive and negative push-offs, respectively. For $\alpha, \beta \in H_1(F)$,

$$\mathcal{G}(\alpha, \beta) = \ell k(\tau\alpha, \beta) = \ell k(i_{+*}(\tau\alpha), \beta) = \frac{1}{2} \ell k(i_{+*}(\tau\alpha), \tau\beta).$$

For homology classes $[a], [b] \in H_1(\Sigma)$, we use $[a] \cdot [b]$ to denote their algebraic intersection, and below we apply Equation (4) to the curves $i_{-*}(\tau\alpha)$ and $\tau\beta$ to the second line to see that

$$\begin{aligned} \mathcal{G}(\alpha, \beta) - \mathcal{G}(\beta, \alpha) &= \frac{1}{2} \ell k(i_{+*}(\tau\alpha), \tau\beta) - \frac{1}{2} \ell k(i_{+*}(\tau\beta), \tau\alpha) \\ &= \frac{1}{2} \ell k(i_{+*}(\tau\alpha), \tau\beta) - \frac{1}{2} \ell k(\tau\beta, i_{-*}(\tau\alpha)) \\ &= \frac{1}{2} \ell k(i_{+*}(\tau\alpha), \tau\beta) - \frac{1}{2} \ell k(i_{-*}(\tau\alpha), \tau\beta) - \frac{1}{2} [\tau\alpha] \cdot [\tau\beta] \\ &= \frac{1}{2} \ell k(i_{+*}(\tau\alpha) - i_{-*}(\tau\alpha), \tau\beta) - \frac{1}{2} [\tau\alpha] \cdot [\tau\beta] \\ &= \left(\frac{1}{2} \tau\alpha \cdot \tau\beta + \frac{1}{2} [\tau\alpha] \cdot [\tau\beta] \right) - \frac{1}{2} [\tau\alpha] \cdot [\tau\beta] = 0. \end{aligned}$$

The term $\tau\alpha \cdot \tau\beta$ in the last step refers to the intersection product of curves on \tilde{F} . Since each point of $\alpha \cdot \beta$ gives rise to two pairs of points in $\tau\alpha \cdot \tau\beta$ of opposite signs, it follows that $\tau\alpha \cdot \tau\beta = 0$, and this completes the proof of the lemma. \square

Lemma 6.5. For some choice of basis $\alpha_1, \dots, \alpha_n$ for $H_1(F)$, the matrix representative of the pairing $\mathcal{G}_F: H_1(F) \times H_1(F) \rightarrow \mathbb{Z}$ is the Goeritz matrix $G_\xi(D) = (g_{ij})$ of Definition 6.1.

Proof. The first step is to construct a spanning surface F for D using the black regions of the checkerboard coloring. Thus F is a union of disks and bands, with one disk for each

black region and one half-twisted band for each crossing $c \in C_D$. In constructing F in $\Sigma \times I$, we can assume that each disk lies in $\Sigma \times \{1/2\}$.

We embed a graph Γ in $F \cap (\Sigma \times \{1/2\})$ with one vertex for each disk and one edge for each band. Notice that Γ is a deformation retract of F . We label the regions of $\Sigma \setminus \Gamma$ as Y_0, Y_1, \dots, Y_n so that Y_i contains X_i for $i = 0, \dots, n$. Each Y_i is oriented using the orientation of Σ , and we set $\alpha_i = [\partial Y_i]$, obtaining homology classes which generate $H_1(\Gamma) \cong H_1(F)$ subject to the sole relation $\sum_{i=0}^n \alpha_i = 0$.

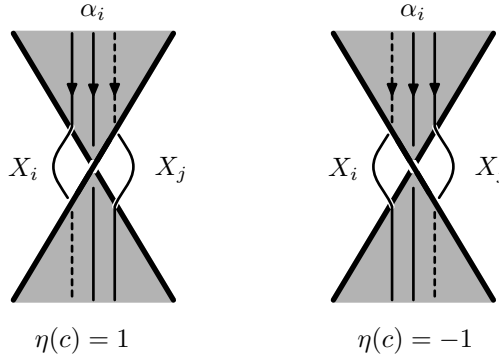


FIGURE 14. Double points c contribute with sign $\eta(c)$.

Since $\sum_{j=0}^n \alpha_j = 0$ and $\sum_{j=0}^n g_{ij} = 0$, it is enough to show that

$$\mathcal{G}_F(\alpha_i, \alpha_j) = g_{ij} \text{ for } i \neq j.$$

But $\mathcal{G}_F(\alpha_i, \alpha_j) = \ell k(\tau \alpha_i, \alpha_j) = \tau \alpha_i \cdot Y_j$. Notice that $\tau \alpha_i$ intersects Y_j only near double points incident to both X_i and X_j , and each such double point c contributes with sign $\eta(c)$, see Figure 14. \square

For a diagram D with checkerboard coloring ξ , we say a crossing $c \in C_D$ is type I or type II according to Figure 15. Notice that the spanning surface F defined by the black regions is orientable if and only if every crossing is of type I.

Proposition 6.6. *If K is an almost classical knot, then it can be represented by a virtual knot diagram D whose Carter surface is minimal genus and which admits a checkerboard coloring ξ so that every crossing has type I.*

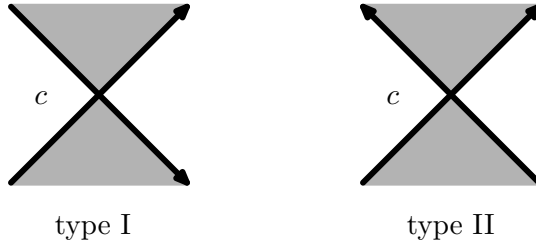


FIGURE 15. Two types of crossings.

Proof. If D is a minimal crossing diagram for K , then by parity, it follows that D is Alexander numberable and that its Carter surface has minimal genus. Notice further that a diagram is checkerboard colorable if and only if it is mod 2 Alexander numberable, and thus D is checkerboard colorable.

By [BGH⁺17], a knot diagram D in $\Sigma \times I$ is Alexander numberable if and only if it bounds an orientable surface, and we apply Seifert's construction to build a Seifert surface F for D in $\Sigma \times I$. The surface F can be realized as a union of disks and bands. Performing an isotopy of F , we can shrink the disks so their images under projection $\Sigma \times I \rightarrow \Sigma$ are disjoint from one another and also disjoint from each band. The isotopy of F induces an isotopy of the knot diagram, and notice that the new knot diagram may no longer be a minimal crossing diagram for K .

Our goal is to show that this new diagram can be isotoped further so that the Seifert surface coincides with the spanning surface associated to the black regions. (This is equivalent to showing that K can be represented by a special diagram in the sense of [BZH14, Definition 13.14].) By construction, the new diagram bounds a Seifert surface, which projects one-to-one under $\Sigma \times I \rightarrow \Sigma$ except possibly at the intersections of the bands.

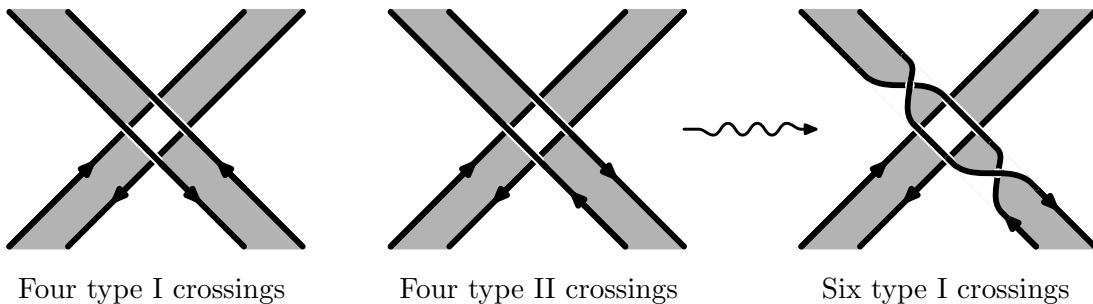


FIGURE 16. Band intersections with all crossings of the same type. An isotopy of the middle diagram gives the one on the right.

Whenever two bands intersect, the four crossings all have the same type, see the two diagrams on the left of Figure 16. If the four crossings have type II, then one can perform a Reidemeister 2 move to make them type I crossings, see the diagram on the right of Figure 16. After performing a finite sequence of such moves, the new knot diagram will have only type I crossings. Consequently the black regions of its associated checkerboard coloring will form an oriented spanning surface, and this completes the proof of the proposition. \square

Theorem 6.7. *Suppose K is an almost classical knot with virtual knot diagram D and checkerboard coloring ξ . Assume further that every crossing has type I (see Figure 15). Then \mathcal{G}_F is represented by the symmetric matrix $V^+ + (V^+)^{\tau}$, where F is the oriented spanning surface obtained from the black regions and V^+ is the associated Seifert matrix obtained by taking the positive push-offs.*

Proof. Since F is orientable, $\tau\alpha = i_{+*}(\alpha) + i_{-*}(\alpha)$. Thus

$$\begin{aligned} \mathcal{G}_F(\alpha, \beta) &= \ell k(\tau\alpha, \beta) \\ &= \ell k(i_{+*}(\alpha), \beta) + \ell k(i_{-*}(\alpha), \beta) \\ &= \ell k(i_{+*}(\alpha), \beta) + \ell k(\alpha, i_{+*}(\beta)) \end{aligned}$$

Given a basis $\alpha_1, \dots, \alpha_{2g}$ for $H_1(F)$, the Seifert matrix V^+ has (i, j) entry given by $\ell k(\alpha_i^+, \alpha_j)$, and $(V^+)^{\tau}$ has (i, j) entry given by $\ell k(\alpha_j, \alpha_i^+)$.

Thus

$$\mathcal{G}_F(\alpha_i, \alpha_j) = \ell k(i_{+*}(\alpha_i), \alpha_j) + \ell k(\alpha_i, i_{+*}(\alpha_j)) = V_{ij}^+ + (V^+)^{\tau}_{ij}.$$

□

Corollary 6.8. *Under the same assumptions, the signature $\sigma(K, F)$ and nullity $n(K, F)$ equal the signature and nullity of the Goeritz matrix $G_{\xi}(D)$.*

The following is a consequence of the result in [ILL10] where they show that the signature and nullity of the modified Goeritz matrix take on at most one of two possible values, depending only on the choice ξ of checkerboard coloring.

Corollary 6.9. *For any almost classical knot and Seifert surface F , the signature $\sigma(K, F)$ and nullity $n(K, F)$ take on one of two possible values.*

Acknowledgements. We would like to thank Andrew Nicas and Robb Todd for useful discussions. H. Boden was supported by a grant from the Natural Sciences and Engineering Research Council of Canada, M. Chrisman was supported by a Monmouth University Creativity and Research Grant, and R. Gaudreau was supported by a scholarship from the National Centre of Competence in Research SwissMAP.

REFERENCES

- [BCG17a] Hans U. Boden, Micah Chrisman, and Robin Gaudreau, *Virtual knot cobordism and bounding the slice genus*, 2017. ArXiv/1708.05982.
- [BCG17b] ———, *Virtual slice genus tables*, 2017. micah46.wixsite.com/micahknots/slicegenus.
- [BGH⁺17] Hans U. Boden, Robin I. Gaudreau, Eric Harper, Andrew J. Nicas, and Lindsay White, *Virtual knot groups and almost classical knots*, *Fundamenta Mathematicae* **138** (2017), 101–142.
- [BN17] Hans U. Boden and Matthias Nagel, *Concordance group of virtual knots*, *Proc. Amer. Math. Soc.* (2017). to appear.
- [BZH14] Gerhard Burde, Heiner Zieschang, and Michael Heusener, *Knots*, extended, De Gruyter Studies in Mathematics, vol. 5, De Gruyter, Berlin, 2014. MR3156509
- [Car91] J. Scott Carter, *Classifying immersed curves*, *Proc. Amer. Math. Soc.* **111** (1991), no. 1, 281–287. MR1043406 (91d:57002)
- [Chr17] Micah Chrisman, *Band-passes and long virtual knot concordance*, *J. Knot Theory Ramifications* (2017), 1750057.
- [CKS02] J. Scott Carter, Seiichi Kamada, and Masahico Saito, *Stable equivalence of knots on surfaces and virtual knot cobordisms*, *J. Knot Theory Ramifications* **11** (2002), no. 3, 311–322. Knots 2000 Korea, Vol. 1 (Yongpyong). MR1905687 (2003f:57011)
- [CSW⁺09] J. Scott Carter, Daniel S. Silver, Susan G. Williams, Mohamed Elhamdadi, and Masahico Saito, *Virtual knot invariants from group biquandles and their cocycles*, *J. Knot Theory Ramifications* **18** (2009), no. 7, 957–972. MR2549477 (2010i:57026)
- [CT07] David Cimasoni and Vladimir Turaev, *A generalization of several classical invariants of links*, *Osaka J. Math.* **44** (2007), no. 3, 531–561. MR2360939
- [DKK17] Heather A. Dye, Aaron Kaestner, and Louis H. Kauffman, *Khovanov homology, Lee homology and a Rasmussen invariant for virtual knots*, *J. Knot Theory Ramifications* **26** (2017), no. 3, 1741001, 57. MR3627701
- [Fox62] R. H. Fox, *Some problems in knot theory*, Topology of 3-manifolds and related topics (Proc. The Univ. of Georgia Institute, 1961), 1962, pp. 168–176. MR0140100
- [Gil82] Cole A. Giller, *A family of links and the Conway calculus*, *Trans. Amer. Math. Soc.* **270** (1982), no. 1, 75–109. MR642331
- [GL78] C. McA. Gordon and R. A. Litherland, *On the signature of a link*, *Invent. Math.* **47** (1978), no. 1, 53–69. MR0500905

- [GPV00] Mikhael Goussarov, Michael Polyak, and Oleg Viro, *Finite-type invariants of classical and virtual knots*, Topology **39** (2000), no. 5, 1045–1068. MR1763963 (2001i:57017)
- [Gre04] Jeremy Green, *A table of virtual knots*, 2004. www.math.toronto.edu/drorbn/Students/GreenJ.
- [ILL10] Young Ho Im, Kyeonghui Lee, and Sang Youl Lee, *Signature, nullity and determinant of checkerboard colorable virtual links*, J. Knot Theory Ramifications **19** (2010), no. 8, 1093–1114. MR2718629
- [Kam02] Naoko Kamada, *On the Jones polynomials of checkerboard colorable virtual links*, Osaka J. Math. **39** (2002), no. 2, 325–333. MR1914297
- [Kau15] Louis Hirsch Kauffman, *Virtual knot cobordism*, New ideas in low dimensional topology, 2015, pp. 335–377. MR3381329
- [Kau99] Louis H. Kauffman, *Virtual knot theory*, European J. Combin. **20** (1999), no. 7, 663–690. MR1721925 (2000i:57011)
- [Kaw96] Akio Kawauchi, *A survey of knot theory*, Birkhäuser Verlag, Basel, 1996. Translated and revised from the 1990 Japanese original by the author. MR1417494
- [KK00] Naoko Kamada and Seiichi Kamada, *Abstract link diagrams and virtual knots*, J. Knot Theory Ramifications **9** (2000), no. 1, 93–106. MR1749502 (2001h:57007)
- [Lic97] W. B. Raymond Lickorish, *An introduction to knot theory*, Graduate Texts in Mathematics, vol. 175, Springer-Verlag, New York, 1997. MR1472978
- [Man07] V. O. Manturov, *Khovanov’s homology for virtual knots with arbitrary coefficients*, Izv. Ross. Akad. Nauk Ser. Mat. **71** (2007), no. 5, 111–148. MR2362875
- [Man10] Vassily O. Manturov, *Parity in knot theory*, Mat. Sb. **201** (2010), no. 5, 65–110. MR2681114
- [Nik13] Igor M. Nikonorov, *Weak parities and functional maps*, Sovrem. Mat. Fundam. Napravl. **51** (2013), 123–141. J. Math. Sci. (N.Y.) **214** (2016), no. 5 699–717. MR3527973
- [Pol10] Michael Polyak, *Minimal generating sets of Reidemeister moves*, Quantum Topol. **1** (2010), no. 4, 399–411. MR2733246
- [SW06] Daniel S. Silver and Susan G. Williams, *Crowell’s derived group and twisted polynomials*, J. Knot Theory Ramifications **15** (2006), no. 8, 1079–1094. MR2275098 (2008i:57011)
- [Tur08] Vladimir Turaev, *Cobordism of knots on surfaces*, J. Topol. **1** (2008), no. 2, 285–305. MR2399131

7. TABLES

Below are several figures and tables of almost classical knots with up to six crossings. Figure 17 shows all the slice almost classical knots, with the slicing indicated as a saddle move on the Gauss diagram. Table 1 gives their Alexander-Conway polynomials and Table 2 shows their graded genus, signature, ω -signatures, and slice genus. Figure 18 gives realizations of each almost classical knot as a knot in a thickened surface. The knot diagrams determine Seifert surfaces in the usual way, and the resulting pairs of Seifert matrices are listed in Table 3.

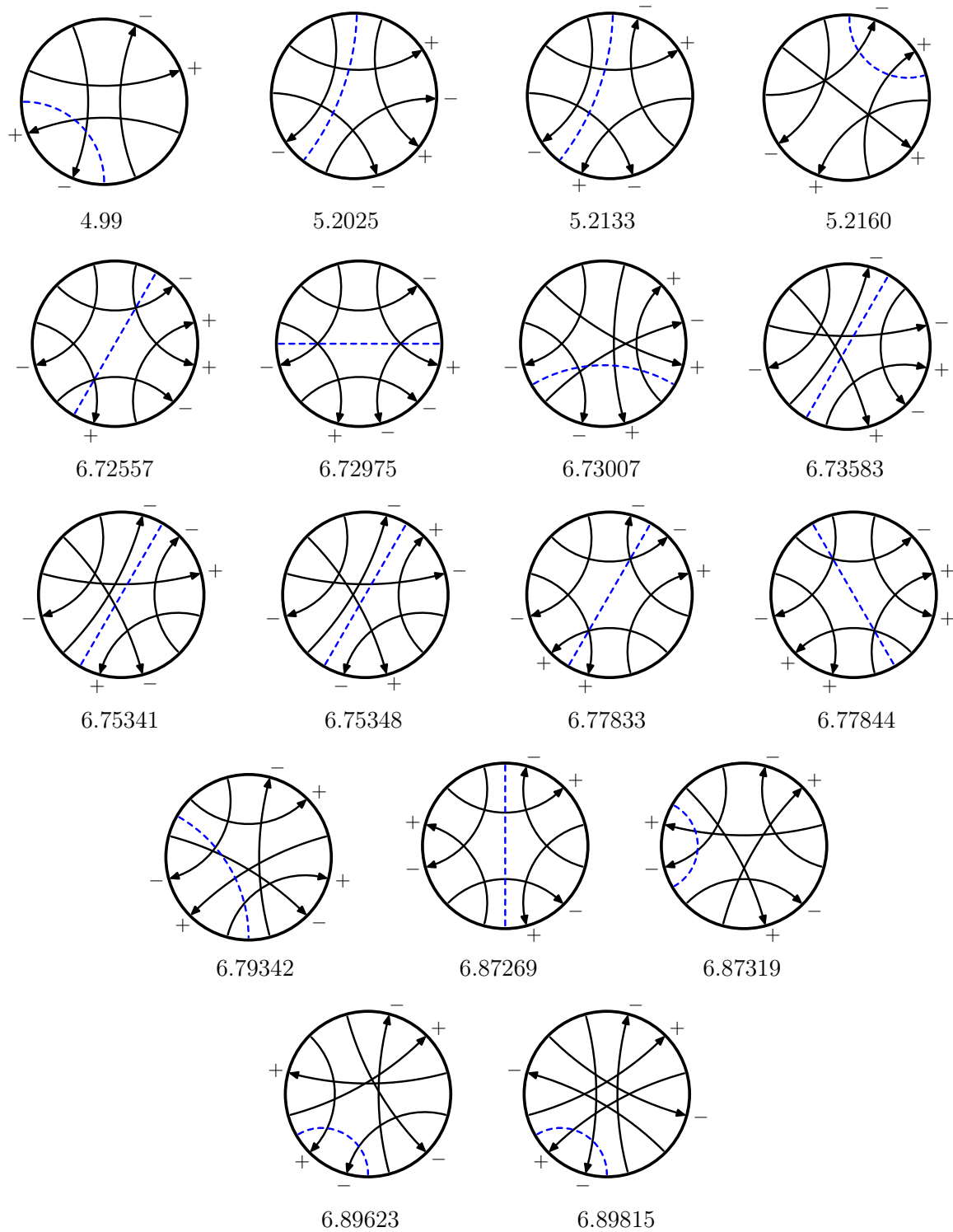


FIGURE 17. SLICE GAUSS DIAGRAMS OF ALMOST CLASSICAL KNOTS

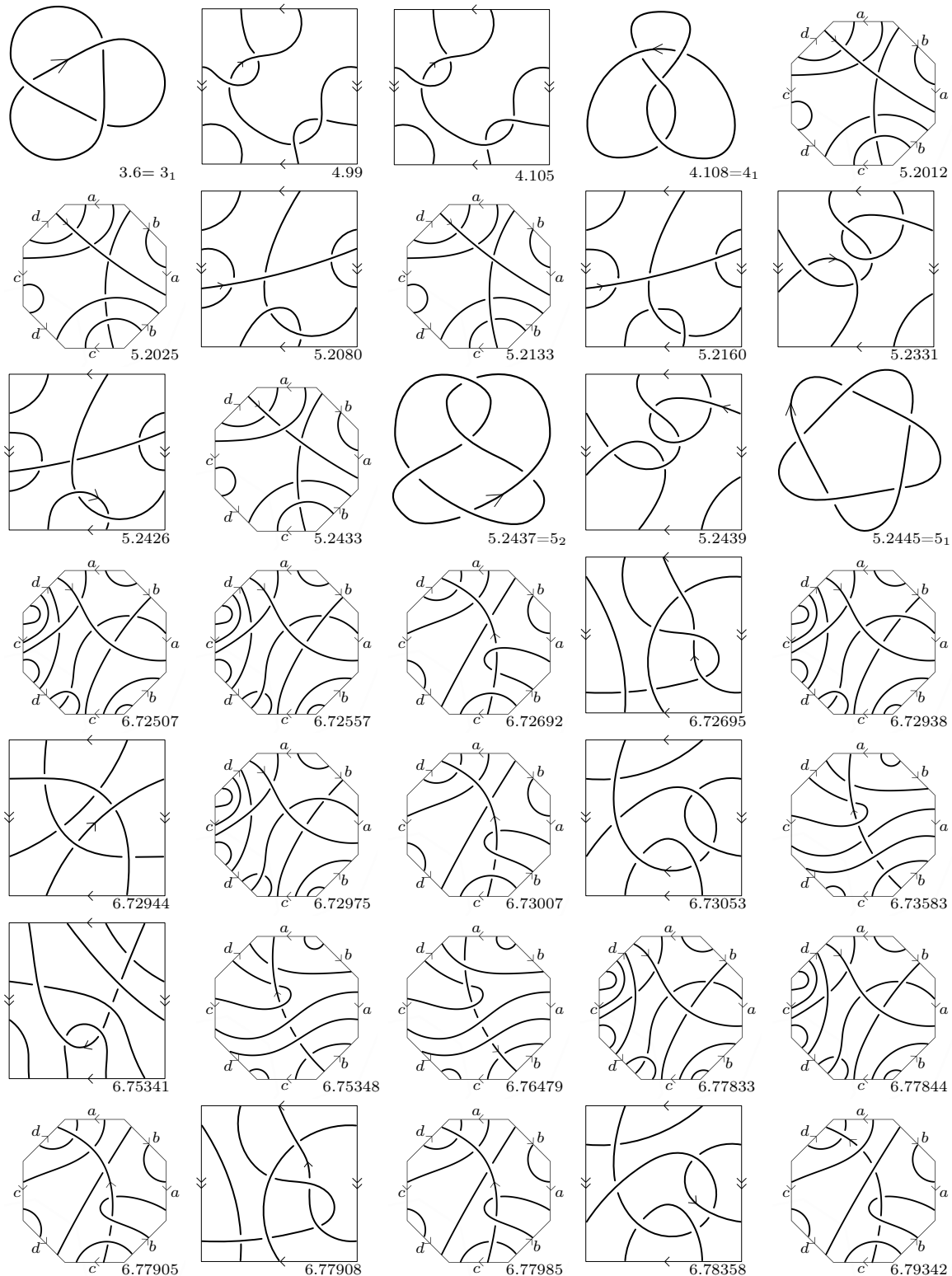
Virtual Knot	Alexander Conway polynomial	Virtual Knot	Alexander Conway polynomial
u3.6	$t - 1 + t^{-1}$	6.85774	$t - 1 + t^{-2}$
4.99	$2 - t^{-1}$	6.87188	$2t - 3 + 3t^{-1} - t^{-2}$
4.105	$2t - 2 + t^{-1}$	6.87262	$t^3 - 2t^2 + 3t - 2 + t^{-1}$
u4.108	$t - 3 + t^{-1}$	6.87269	$4 - 4t^{-1} + t^{-2}$
5.2012	t	6.87310	$t^2 - t + 2 - 2t^{-1} + t^{-2}$
5.2025	t	6.87319	$3 - 3t^{-1} + t^{-2}$
5.2080	1	6.87369	$t - 2 + 3t^{-1} - t^{-2}$
5.2133	$2 - t^{-1}$	6.87548	$-t^2 + 2t + 1 - t^{-1}$
5.2160	$t - 1 + t^{-1}$	6.87846	$t - 1 + 2t^{-1} - t^{-2}$
5.2331	$t^2 - 1 + t^{-1}$	6.87857	$-t + 4 - 2t^{-1}$
5.2426	$(t - 1 + t^{-1})^2$	6.87859	$3 - 3t^{-1} + t^{-2}$
5.2433	$t^2 - 2t + 4 - 3t^{-1} + t^{-2}$	6.87875	$t + 1 - 2t^{-1} + t^{-2}$
u5.2437	$2t - 3 + 2t^{-1}$	6.89156	$2t - 1 - t^{-1} + t^{-2}$
5.2439	$t^2 - 2t + 3 - t^{-1}$	u6.89187	$(t - 1 + t^{-1})^2$
u5.2445	$t^2 - t + 1 - t^{-1} + t^{-2}$	u6.89198	$(t - 1 + t^{-1})^2$
6.72507	t	6.89623	$2 - 2t^{-1} + t^{-2}$
6.72557	t	6.89812	$t^2 - 2 + 2t^{-1}$
6.72692	1	6.89815	$2t^{-1} - t^{-2}$
6.72695	t	6.90099	$t - t^{-1} + t^{-3}$
6.72938	$t^2 - t + 1$	6.90109	$2t^2 - 4t + 5 - 3t^{-1} + t^{-2}$
6.72944	$2t - 1$	6.90115	$-t^2 + 4t + -5 + 4t^{-1} - t^{-2}$
6.72975	t	6.90139	$3t^2 - 6t + 7 - 4t^{-1} + t^{-2}$
6.73007	1	6.90146	$t^3 - 5t^2 + 9t - 5 + t^{-1}$
6.73053	$t - 1 + t^{-1}$	6.90147	$t^2 - 3t + 6 - 5t^{-1} + 2t^{-2}$
6.73583	1	6.90150	$-t^2 + 5t - 6 + 4t^{-1} - t^{-2}$
6.75341	$2 - t^{-1}$	6.90167	$t^2 - 2t + 4 - 4t^{-1} + 2t^{-2}$
6.75348	$-t^2 + 2t$	u6.90172	$t^2 - 3t + 5 - 3t^{-1} + t^{-2}$
6.76479	$t - 1 + t^{-1}$	6.90185	$3t^2 - 6t + 6 - 3t^{-1} + t^{-2}$
6.77833	$t^2 - t + 1$	6.90194	$t^2 - 4t + 8 - 5t^{-1} + t^{-2}$
6.77844	$t^2 - t + 1$	6.90195	$2t^2 - 3t + 3 - 2t^{-1} + t^{-2}$
6.77905	$-t + 3 - t^{-1}$	u6.90209	$t^2 - 3t + 3 - 3t^{-1} + t^{-2}$
6.77908	$2t - 2 + t^{-1}$	6.90214	$3t - 4 + 2t^{-1}$
6.77985	$t - 1 + t^{-1}$	6.90217	$-t^2 + 4t - 3 + t^{-1}$
6.78358	$-t + 3 - t^{-1}$	6.90219	$2t - 3 + 3t^{-1} - t^{-2}$
6.79342	$-t + 3 - t^{-1}$	u6.90227	$2t - 3 + 2t^{-1}$
6.85091	$1 + t^{-1} - t^{-2}$	6.90228	$4t - 6 + 3t^{-1}$
6.85103	$t - 1 + 2t^{-1} - t^{-2}$	6.90232	$-2t + 6 - 4t^{-1} + t^{-2}$
6.85613	$t - 2 + 2t^{-1}$	6.90235	$t - 3 + 5t^{-1} - 3t^{-2} + t^{-3}$

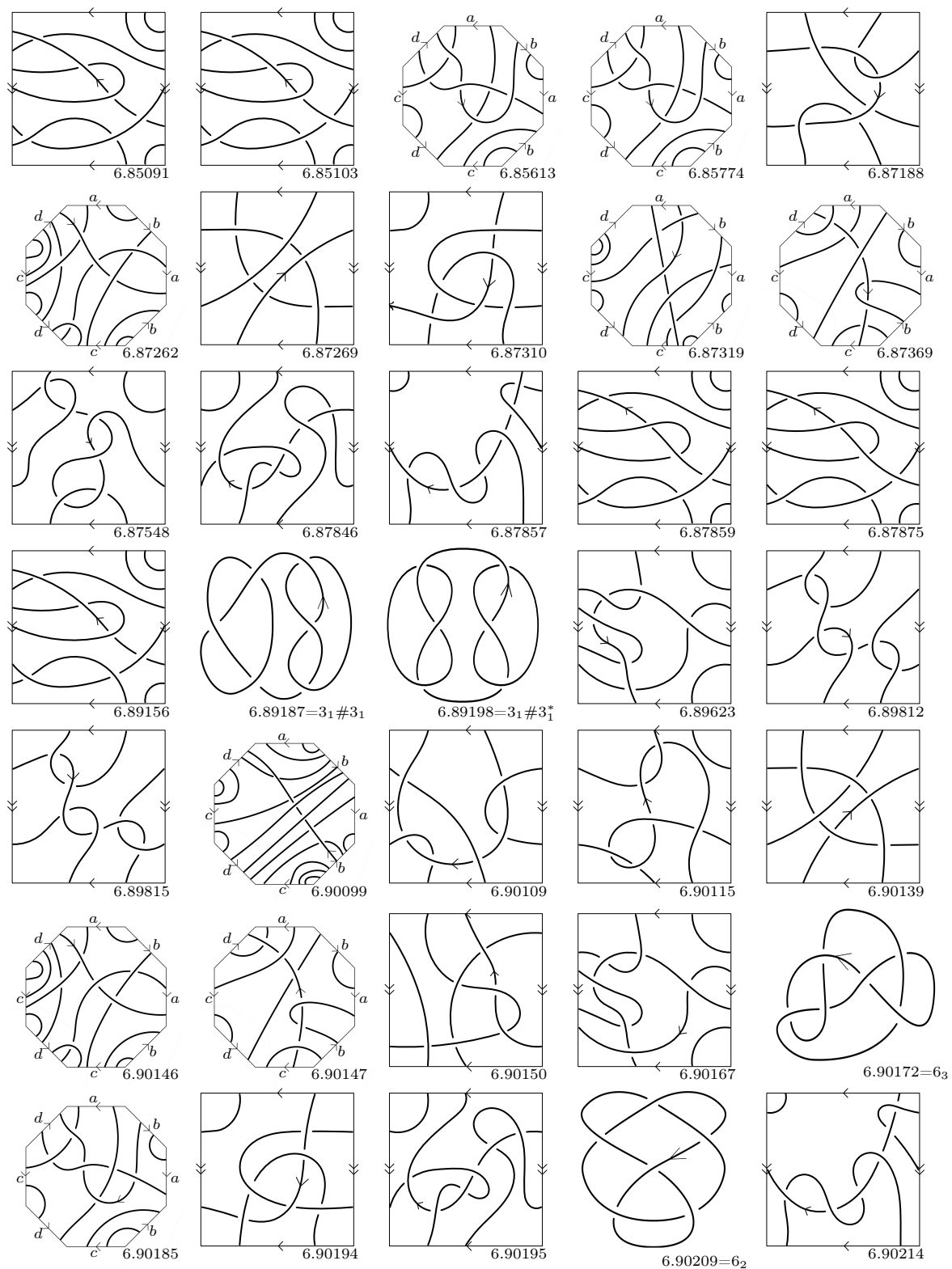
TABLE 1. The Alexander–Conway polynomials of almost classical knots.

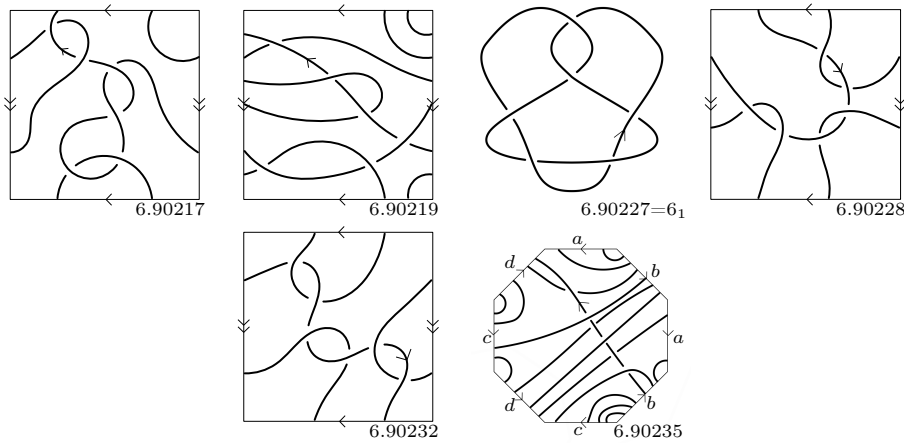
Virtual knot	Graded genus	Signatures σ $\{\hat{\sigma}_\omega^\pm\}$	Slice genus	Virtual knot	Graded genus	Signatures σ $\{\hat{\sigma}_\omega^\pm\}$	Slice genus
u3.6	0	2 $\{0, 2\}$	1	6.85774	1	2 $\{0, 2\}$	1
4.99	0	0 $\{0\}$	0	6.87188	1	2 $\{0, 2\}$	1
4.105	1	2 $\{2\}$	1	6.87262	2	2 $\{0, 2\}$	2
u4.108	0	0 $\{0\}$	1	6.87269	0	0 $\{0\}$	0
5.2012	1	2 $\{0, 2\}$	1	6.87310	1	4 $\{2, 4\}$	2
5.2025	0	0 $\{0\}$	0	6.87319	0	0 $\{0\}$	0
5.2080	1	2 $\{0, 2\}$	1	6.87369	1	-2 $\{-2, 0\}$	1
5.2133	0	0 $\{0\}$	0	6.87548	0	0 $\{0\}$	1
5.2160	0	0 $\{0\}$	0	6.87846	1	2 $\{0, 2\}$	1
5.2331	1	2 $\{2\}$	1	6.87857	1	0 $\{0\}$	1
5.2426	1	4 $\{0, 2, 4\}$	2	6.87859	1	0 $\{-2, 0\}$	1
5.2433	2	4 $\{0, 2, 4\}$	2	6.87875	1	-1 $\{-2, 0\}$	1
u5.2437	0	2 $\{0, 2\}$	1	6.89156	1	2 $\{0, 2\}$	1
5.2439	0	0 $\{0\}$	1	u6.89187	0	4 $\{0, 4\}$	2
u5.2445	0	4 $\{0, 2, 4\}$	2	u6.89198	0	0 $\{0\}$	0
6.72507	1	2 $\{0, 2\}$	1	6.89623	0	0 $\{0\}$	0
6.72557	0	0 $\{0\}$	0	6.89812	1	2 $\{0, 2\}$	1
6.72692	1	2 $\{2\}$	1	6.89815	0	0 $\{0\}$	0
6.72695	0	0 $\{0\}$	1	6.90099	2	2 $\{0, 2\}$	1
6.72938	1	2 $\{0, 2\}$	1	6.90109	1	4 $\{0, 2, 4\}$	2
6.72944	0	2 $\{0, 2\}$	1	6.90115	0	2 $\{0, 2\}$	1 or 2
6.72975	0	0 $\{0\}$	0	6.90139	1	4 $\{0, 2, 4\}$	2
6.73007	0	0 $\{0\}$	0	6.90146	0	2 $\{0, 2\}$	1 or 2
6.73053	1	2 $\{0, 2\}$	1	6.90147	2	4 $\{2, 4\}$	2
6.73583	0	1 $\{1\}$	0	6.90150	0	2 $\{0, 2\}$	1 or 2
6.75341	0	0 $\{0\}$	0	6.90167	1	4 $\{0, 2, 4\}$	2
6.75348	0	1 $\{0\}$	0	u6.90172	0	0 $\{0\}$	1
6.76479	1	2 $\{2\}$	1	6.90185	2	4 $\{0, 2, 4\}$	2
6.77833	0	0 $\{0\}$	0	6.90194	0	0 $\{0\}$	1 or 2
6.77844	0	0 $\{0\}$	0	6.90195	1	4 $\{0, 2, 4\}$	2
6.77905	1	1 $\{1\}$	1	u6.90209	0	2 $\{0, 2\}$	1
6.77908	0	-1 $\{-1, 0\}$	1	6.90214	1	2 $\{0, 2\}$	1
6.77985	1	-1 $\{-1\}$	1	6.90217	1	2 $\{0, 2\}$	1
6.78358	1	0 $\{0\}$	1	6.90219	1	2 $\{0, 2\}$	1
6.79342	0	0 $\{0\}$	0	u6.90227	0	0 $\{0\}$	0
6.85091	1	0 $\{0\}$	1	6.90228	1	2 $\{0, 2\}$	1
6.85103	0	-1 $\{0\}$	1	6.90232	1	0 $\{0\}$	1
6.85613	1	2 $\{0, 2\}$	1	6.90235	0	-2 $\{-2, 0, 2\}$	1

TABLE 2. The graded genus, signature, ω -signatures, and slice genus of almost classical knots.

FIGURE 18. DIAGRAMS OF ALMOST CLASSICAL KNOTS IN SURFACES







Knot	Seifert matrices
u3.6	$V^+ = [[1, -1], [0, 1]]$ $V^- = [[1, 0], [-1, 1]]$
4.99	$V^+ = [[-1, 0], [0, 1]]$ $V^- = [[-1, 1], [-1, 1]]$
4.105	$V^+ = [[1, 0], [0, 1]]$ $V^- = [[1, 1], [-1, 1]]$
u4.108	$V^+ = [[-1, 0], [1, 1]]$ $V^- = [[-1, 1], [0, 1]]$
5.2012	$V^+ = [[0, 0, -1, 1], [0, 1, 0, 0], [0, 0, 0, 0], [0, -1, 0, 1]]$ $V^- = [[0, -1, -1, 1], [1, 1, 1, 0], [0, -1, 0, 1], [0, -1, -1, 1]]$
5.2025	$V^+ = [[0, 0, -1, 1], [0, 1, 0, 1], [0, 0, 0, 0], [0, 0, 0, 0]]$ $V^- = [[0, -1, -1, 1], [1, 1, 1, 1], [0, -1, 0, 1], [0, 0, -1, 0]]$
5.2080	$V^+ = [[1, 1, 0, 0], [0, 0, 0, 0], [0, 0, 1, 1], [-1, 0, 0, 1]]$ $V^- = [[1, 0, 0, -1], [1, 0, 0, -1], [0, 0, 1, 0], [0, 1, 1, 1]]$
5.2133	$V^+ = [[0, 0, -1, 1], [0, 1, 0, 0], [0, 0, -1, 0], [0, -1, 0, 1]]$ $V^- = [[0, -1, -1, 1], [1, 1, 1, 0], [0, -1, -1, 1], [0, -1, -1, 1]]$
5.2160	$V^+ = [[-1, 0, 0, 1], [-1, -1, 0, 0], [0, 0, 1, 1], [0, 0, 0, 0]]$ $V^- = [[-1, -1, 0, 0], [0, -1, 0, -1], [0, 0, 1, 0], [1, 1, 1, 0]]$
5.2331	$V^+ = [[1, 1, 0, 0], [-1, 0, 1, 0], [0, 0, 1, 0], [0, 0, -1, 1]]$ $V^- = [[1, 0, 0, 0], [0, 0, 0, 0], [0, 1, 1, -1], [0, 0, 0, 1]]$
5.2426	$V^+ = [[1, 1, 0, 0], [0, 1, 0, 0], [0, 0, 1, 1], [-1, 0, 0, 1]]$ $V^- = [[1, 0, 0, -1], [1, 1, 0, -1], [0, 0, 1, 0], [0, 1, 1, 1]]$
5.2433	$V^+ = [[1, 0, 0, 1], [0, 1, 0, 0], [1, 0, 1, 0], [0, -1, 0, 1]]$ $V^- = [[1, -1, 0, 1], [1, 1, 1, 0], [1, -1, 1, 1], [0, -1, -1, 1]]$
u5.2437	$V^+ = [[2, -2], [-1, 2]]$ $V^- = [[2, -1], [-2, 2]]$
5.2439	$V^+ = [[-1, 1, 0, 0], [-1, 0, 1, 0], [0, 0, 1, 0], [0, 0, -1, 1]]$ $V^- = [[-1, 0, 0, 0], [0, 0, 0, 0], [0, 1, 1, -1], [0, 0, 0, 1]]$
u5.2445	$V^+ = [[1, 0, -1, 0], [0, 1, 0, -1], [0, 0, 1, 0], [-1, 0, 0, 1]]$ $V^- = [[1, 0, 0, -1], [0, 1, 0, 0], [-1, 0, 1, 0], [0, -1, 0, 1]]$

Knot	Seifert matrices
6.72557	$V^+ = [[0, 1, 0, 0, 0, 0], [0, 1, 0, 0, 0, 0], [1, 1, 0, -1, 1, 1], [0, 0, 0, -1, 1, 0], [0, 0, 0, 0, 0, 0], [0, 0, 0, 0, 0, 0]]$ $V^- = [[0, 1, 1, 0, 0, 0], [0, 1, 1, 0, 0, -1], [0, 0, 0, 0, 0, 0], [0, 0, -1, -1, 0, 0], [0, 0, 1, 1, 0, -1], [0, 1, 1, 0, 1, 0]]$
6.72692	$V^+ = [[1, 1, 1, 1], [-1, 0, -1, 0], [-1, 0, 0, 0], [-1, 1, 0, 1]]$ $V^- = [[1, 0, 0, 0], [0, 0, -1, 1], [0, 0, 0, 0], [0, 0, 0, 1]]$
6.72695	$V^+ = [[0, 1, 0, 0], [0, -1, 0, 0], [1, 1, 1, 1], [-1, 1, -1, 0]]$ $V^- = [[0, 0, 0, 0], [1, -1, 1, 1], [1, 0, 1, 0], [-1, 0, 0, 0]]$
6.72938	$V^+ = [[1, 1, 0, 0, 0, 0], [0, 1, 0, 0, 0, 0], [1, 1, 1, 0, 1, 1], [0, 0, 1, 0, 1, 0], [0, 0, 0, 0, 0, 0], [0, 0, 0, 0, 0, 0]]$ $V^- = [[1, 1, 1, 0, 0, 0], [0, 1, 1, 0, 0, -1], [0, 0, 1, 1, 0, 0], [0, 0, 0, 0, 0, 0], [0, 0, 1, 1, 0, -1], [0, 1, 1, 0, 1, 0]]$
6.72944	$V^+ = [[-1, -1, 0, 0], [0, 0, 0, 0], [0, 0, 1, 0], [0, 0, 1, 1]]$ $V^- = [[-1, -1, 0, -1], [0, 0, 1, 0], [0, -1, 1, 0], [1, 0, 1, 1]]$
6.72975	$V^+ = [[0, 1, 0, 0, 0, 0], [0, 1, 0, 0, 0, 0], [1, 1, 1, 0, 1, 1], [0, 0, 1, 0, 1, 0], [0, 0, 0, 0, 0, 0], [0, 0, 0, 0, 0, 0]]$ $V^- = [[0, 1, 1, 0, 0, 0], [0, 1, 1, 0, 0, -1], [0, 0, 1, 1, 0, 0], [0, 0, 0, 0, 0, 0], [0, 0, 1, 1, 0, -1], [0, 1, 1, 0, 1, 0]]$
6.73007	$V^+ = [[-1, 1, 1, 1], [-1, 0, -1, 0], [-1, 0, 0, 0], [-1, 1, 0, 1]]$ $V^- = [[-1, 0, 0, 0], [0, 0, -1, 1], [0, 0, 0, 0], [0, 0, 0, 1]]$
6.73053	$V^+ = [[1, 0, 1, 0], [-1, 1, 0, 0], [-1, 1, 0, 1], [0, 0, 0, 1]]$ $V^- = [[1, -1, 0, 0], [0, 1, 1, 0], [0, 0, 0, 0], [0, 0, 1, 1]]$
6.73583	$V^+ = [[1, 0, 0, 0], [0, 0, 0, 0], [0, 0, 0, -1], [0, 1, 0, 0]]$ $V^- = [[1, -1, 1, 0], [1, 0, 0, 1], [-1, 0, 0, -1], [0, 0, 0, 0]]$
6.75341	$V^+ = [[0, 1, 1, 1], [-1, 0, 1, 0], [0, 0, 1, 0], [0, -1, 0, -1]]$ $V^- = [[0, 0, 0, 0], [0, 0, 0, 0], [1, 1, 1, 0], [1, -1, 0, -1]]$
6.75348	$V^+ = [[1, 0, 0, 0], [0, 0, 0, -1], [0, 0, 0, -1], [0, 0, 0, -1]]$ $V^- = [[1, -1, 1, 0], [1, 0, 0, 0], [-1, 0, 0, -1], [0, -1, 0, -1]]$
6.76479 ^r	$V^+ = [[1, 0, 0, 0], [0, 0, 0, -1], [0, 0, 1, 0], [0, 0, 1, 0]]$ $V^- = [[1, -1, 1, 0], [1, 0, 0, 0], [-1, 0, 1, 0], [0, -1, 1, 0]]$
6.77833	$V^+ = [[1, 1, 0, 0, 0, 0], [0, 0, 0, 0, 0, 0], [1, 1, 0, -1, 1, 1], [0, 0, 0, -1, 1, 0], [0, 0, 0, 0, 0, 0], [0, 0, 0, 0, 0, 0]]$ $V^- = [[1, 1, 1, 0, 0, 0], [0, 0, 1, 0, 0, -1], [0, 0, 0, 0, 0, 0], [0, 0, -1, -1, 0, 0], [0, 0, 1, 1, 0, -1], [0, 1, 1, 0, 1, 0]]$
6.77844	$V^+ = [[0, 1, 0, 0, 0, 0], [0, 0, 0, 0, 0, 0], [1, 1, 0, -1, 1, 1], [0, 0, 0, -1, 1, 0], [0, 0, 0, 0, 0, 0], [0, 0, 0, 0, 0, 0]]$ $V^- = [[0, 1, 1, 0, 0, 0], [0, 0, 1, 0, 0, -1], [0, 0, 0, 0, 0, 0], [0, 0, -1, -1, 0, 0], [0, 0, 1, 1, 0, -1], [0, 1, 1, 0, 1, 0]]$
6.77905	$V^+ = [[1, 1, 1, 1], [-1, 0, -1, 0], [-1, 0, -1, 0], [-1, 1, 0, 1]]$ $V^- = [[1, 0, 0, 0], [0, 0, -1, 1], [0, 0, -1, 0], [0, 0, 0, 1]]$
6.77908	$V^+ = [[-1, 1, -1, 0], [0, -1, 0, 0], [0, 1, 0, 1], [-1, 1, -1, 0]]$ $V^- = [[-1, 0, -1, 0], [1, -1, 1, 1], [0, 0, 0, 0], [-1, 0, 0, 0]]$
6.77985	$V^+ = [[-1, 1, 1, 1], [-1, 0, -1, 0], [-1, 0, -1, 0], [-1, 1, 0, 1]]$ $V^- = [[-1, 0, 0, 0], [0, 0, -1, 1], [0, 0, -1, 0], [0, 0, 0, 1]]$
6.78358	$V^+ = [[0, 0, 1, 0], [-1, 1, 0, 0], [-1, 1, 0, 1], [0, 0, 0, 1]]$ $V^- = [[0, -1, 0, 0], [0, 1, 1, 0], [0, 0, 0, 0], [0, 0, 1, 1]]$

Knot	Seifert matrices
6.79342	$V^+ = [[-1, 1, 1, 1], [-1, 0, 0, -1], [-1, 1, 1, 0], [-1, 0, 0, 0]]$ $V^- = [[-1, 0, 0, 0], [0, 0, 0, 0], [0, 1, 1, 0], [0, -1, 0, 0]]$
6.85091	$V^+ = [[-1, 0, 0, 0], [0, 1, -1, 0], [0, 1, 0, 1], [0, 0, 0, 1]]$ $V^- = [[-1, 1, 0, 0], [-1, 1, 0, 0], [0, 0, 0, 0], [0, 0, 1, 1]]$
6.85103	$V^+ = [[-1, 0, 0, 0], [0, 0, -1, 0], [0, 1, 0, 1], [0, 0, 0, 1]]$ $V^- = [[-1, 1, 0, 0], [-1, 0, 0, 0], [0, 0, 0, 0], [0, 0, 1, 1]]$
6.85613	$V^+ = [[0, 0, 0, 1], [-1, 0, -1, 0], [0, 1, 1, 0], [-1, 0, -1, 1]]$ $V^- = [[0, -1, 0, 0], [0, 0, 0, 0], [0, 0, 1, 0], [0, 0, -1, 1]]$
6.85774	$V^+ = [[0, 0, 0, 1], [-1, 1, -1, 0], [0, 1, 1, 0], [-1, 0, -1, 1]]$ $V^- = [[0, -1, 0, 0], [0, 1, 0, 0], [0, 0, 1, 0], [0, 0, -1, 1]]$
6.87188	$V^+ = [[-1, 0, 0, 0], [0, 1, 0, 0], [0, 0, 1, -1], [0, 1, 0, 1]]$ $V^- = [[-1, 1, 0, 0], [-1, 1, -1, 1], [0, 1, 1, 0], [0, 0, -1, 1]]$
6.87262	$V^+ = [[1, 1, 0, 0, 0, 0], [0, 1, 0, 0, 0, 0], [1, 1, 1, 0, 1, 1], [0, 0, 1, 1, 1, 0], [0, 0, 0, 0, 0, 0], [0, 0, 0, 0, 0, 0]]$ $V^- = [[1, 1, 1, 0, 0, 0], [0, 1, 1, 0, 0, -1], [0, 0, 1, 1, 0, 0], [0, 0, 0, 1, 0, 0], [0, 0, 1, 1, 0, -1], [0, 1, 1, 0, 1, 0]]$
6.87269	$V^+ = [[-1, -1, 0, 0], [0, -1, 0, 0], [0, 0, 1, 0], [0, 0, 1, 1]]$ $V^- = [[-1, -1, 0, -1], [0, -1, 1, 0], [0, -1, 1, 0], [1, 0, 1, 1]]$
6.87310	$V^+ = [[1, 1, -1, -1], [0, 1, 0, -1], [0, 0, 1, 1], [0, 0, 0, 1]]$ $V^- = [[1, 1, 0, 0], [0, 1, 0, 0], [-1, 0, 1, 0], [-1, -1, 1, 1]]$
6.87319	$V^+ = [[1, 0, 0, 1], [-1, 1, -1, 0], [0, 1, -1, 1], [-1, 0, 0, -1]]$ $V^- = [[1, -1, 0, 0], [0, 1, 0, 0], [0, 0, -1, 1], [0, 0, 0, -1]]$
6.87369 ^r	$V^+ = [[1, 1, 1, 1], [-1, -1, -1, -1], [-1, 0, -1, 0], [-1, 0, 0, -1]]$ $V^- = [[1, 0, 0, 0], [0, -1, -1, 0], [0, 0, -1, 0], [0, -1, 0, -1]]$
6.87548	$V^+ = [[0, 0, 0, 0], [1, 1, 0, 0], [0, 0, 1, 0], [0, 0, 0, -1]]$ $V^- = [[0, 1, 1, 0], [0, 1, 0, 0], [-1, 0, 1, -1], [0, 0, 1, -1]]$
6.87846	$V^+ = [[1, 1, 0, 0], [0, 1, 0, 0], [-1, 0, 1, 0], [0, 0, 0, -1]]$ $V^- = [[1, 0, -1, 0], [1, 1, 0, -1], [0, 0, 1, 0], [0, 1, 0, -1]]$
6.87857	$V^+ = [[2, 0], [0, -1]]$ $V^- = [[2, 1], [-1, -1]]$
6.87859	$V^+ = [[-1, 0, 0, 0], [0, 1, -1, 0], [0, 1, 0, 1], [0, 0, 0, -1]]$ $V^- = [[-1, 1, 0, 0], [-1, 1, 0, 0], [0, 0, 0, 0], [0, 0, 1, -1]]$
6.87875	$V^+ = [[-1, 0, 0, 0], [0, 0, -1, 0], [0, 1, 0, 1], [0, 0, 0, -1]]$ $V^- = [[-1, 1, 0, 0], [-1, 0, 0, 0], [0, 0, 0, 0], [0, 0, 1, -1]]$
6.89156	$V^+ = [[1, 0, 0, 0], [0, 1, -1, 0], [0, 1, 0, 1], [0, 0, 0, 1]]$ $V^- = [[1, 1, 0, 0], [-1, 1, 0, 0], [0, 0, 0, 0], [0, 0, 1, 1]]$
6.89187	$V^+ = [[1, -1, 0, 0], [0, 1, 0, 0], [0, 0, -1, 1], [0, 0, 0, -1]]$ $V^- = [[1, 0, 0, 0], [-1, 1, 0, 0], [0, 0, -1, 0], [0, 0, 1, -1]]$
6.89198	$V^+ = [[1, -1, 0, 0], [0, 1, 0, 0], [0, 0, 1, 1], [0, 0, 0, 1]]$ $V^- = [[1, 0, 0, 0], [-1, 1, 0, 0], [0, 0, 1, 0], [0, 0, 1, 1]]$
6.89623	$V^+ = [[-1, 0, 0, -1], [0, 1, 0, 0], [0, -1, 1, 0], [0, 0, 0, -1]]$ $V^- = [[-1, -1, 0, 0], [1, 1, -1, 0], [0, 0, 1, 0], [-1, 0, 0, -1]]$
6.89812	$V^+ = [[0, 0, 0, 0], [1, 1, 0, 0], [0, 0, 1, 0], [1, 0, 1, 1]]$ $V^- = [[0, 1, 1, 1], [0, 1, 0, 0], [-1, 0, 1, 1], [0, 0, 0, 1]]$
6.89815 ^r	$V^+ = [[0, 0, 0, 0], [1, -1, 0, 0], [0, 0, 1, 0], [1, 0, 1, 1]]$ $V^- = [[0, 1, 1, 1], [0, -1, 0, 0], [-1, 0, 1, 1], [0, 0, 0, 1]]$
6.90099	$V^+ = [[1, -1, 0, 0, 1, 0], [1, 0, 0, 0, 0, 0], [0, 1, 1, 0, 0, 0], [0, 0, 1, 1, 0, 1], [0, 0, 0, 0, 1, -1], [0, 0, 0, 0, 1, 0]]$ $V^- = [[1, 0, 0, 0, 1, 0], [0, 0, 1, 0, 0, 0], [0, 0, 1, 1, 0, 0], [0, 0, 0, 1, 0, 0], [0, 0, 0, 0, 1, 0], [0, 0, 0, 1, 0, 0]]$

Knot	Seifert matrices
6.90109	$V^+ = [[1, -1, 0, 0], [0, 1, 1, 0], [0, 0, 1, 0], [0, 0, 0, 1]]$ $V^- = [[1, 0, 1, 1], [-1, 1, 0, 0], [-1, 1, 1, 0], [-1, 0, 0, 1]]$
6.90115	$V^+ = [[1, 0, 0, 0], [1, -1, 0, 0], [0, 0, 1, -1], [1, 0, 0, 1]]$ $V^- = [[1, 1, 0, 0], [0, -1, 0, 0], [0, 0, 1, 0], [1, 0, -1, 1]]$
6.90139	$V^+ = [[1, 0, 0, 0], [1, 1, 0, 0], [0, 0, 1, 0], [0, 0, 1, 1]]$ $V^- = [[1, 0, 0, -1], [1, 1, 1, 0], [0, -1, 1, 0], [1, 0, 1, 1]]$
6.90146	$V^+ = [[1, 1, 0, 0, 0, 0], [0, 1, 0, 0, 0, 0], [1, 1, -1, -1, 1, 1], [0, 0, 0, -1, 1, 0], [0, 0, 0, 0, 0, 0], [0, 0, 0, 0, 0, 0]]$ $V^- = [[1, 1, 1, 0, 0, 0], [0, 1, 1, 0, 0, -1], [0, 0, -1, 0, 0, 0], [0, 0, -1, -1, 0, 0], [0, 0, 1, 1, 0, -1], [0, 1, 1, 0, 1, 0]]$
6.90147	$V^+ = [[1, 1, 1, 1], [-1, 1, 0, 0], [-1, 1, 1, 0], [-1, 1, 0, 1]]$ $V^- = [[1, 0, 0, 0], [0, 1, 0, 1], [0, 1, 1, 0], [0, 0, 0, 1]]$
6.90150	$V^+ = [[1, 1, 0, 1], [0, -1, 0, 0], [1, 1, 1, 1], [0, 1, -1, 1]]$ $V^- = [[1, 0, 0, 1], [1, -1, 1, 1], [1, 0, 1, 0], [0, 0, 0, 1]]$
6.90167 ^r	$V^+ = [[1, 0, 0, 0], [0, 1, 0, 0], [0, -1, 1, 0], [1, 0, 0, 1]]$ $V^- = [[1, -1, 0, 1], [1, 1, -1, 0], [0, 0, 1, 0], [0, 0, 0, 1]]$
u6.90172	$V^+ = [[1, -1, 0, 0], [0, 1, 0, 0], [1, -1, -1, 0], [-1, 1, 1, -1]]$ $V^- = [[1, 0, 1, -1], [-1, 1, -1, 1], [0, 0, -1, 1], [0, 0, 0, -1]]$
6.90185 ^r	$V^+ = [[1, 0, 0, 1], [-1, 1, -1, 0], [0, 1, 1, 0], [-1, 0, -1, 1]]$ $V^- = [[1, -1, 0, 0], [0, 1, 0, 0], [0, 0, 1, 0], [0, 0, -1, 1]]$
6.90194	$V^+ = [[-1, 0, -1, -1], [-1, -1, 0, -1], [0, 0, 1, 1], [0, 0, 0, 1]]$ $V^- = [[-1, 0, 0, 0], [-1, -1, 0, 0], [-1, 0, 1, 0], [-1, -1, 1, 1]]$
6.90195	$V^+ = [[1, 1, 0, 0], [0, 1, 0, 0], [-1, 0, 1, 0], [0, 0, 0, 1]]$ $V^- = [[1, 0, -1, 0], [1, 1, 0, -1], [0, 0, 1, 0], [0, 1, 0, 1]]$
u6.90209	$V^+ = [[1, 0, -1, 0], [0, 1, 0, 0], [0, -1, 1, 0], [-1, 0, 1, -1]]$ $V^- = [[1, 0, 0, -1], [0, 1, -1, 0], [-1, 0, 1, 1], [0, 0, 0, -1]]$
6.90214	$V^+ = [[2, 0], [0, 1]]$ $V^- = [[2, 1], [-1, 1]]$
6.90217	$V^+ = [[0, 0, 0, 0], [1, -1, 0, 0], [0, 0, 1, 0], [0, 0, 0, 1]]$ $V^- = [[0, 1, 1, 0], [0, -1, 0, 0], [-1, 0, 1, -1], [0, 0, 1, 1]]$
6.90219	$V^+ = [[1, 0, 0, 0], [0, 1, -1, 0], [0, 1, 0, 1], [0, 0, 0, -1]]$ $V^- = [[1, 1, 0, 0], [-1, 1, 0, 0], [0, 0, 0, 0], [0, 0, 1, -1]]$
u6.90227	$V^+ = [[-1, 0], [1, 2]]$ $V^- = [[-1, 1], [0, 2]]$
6.90228	$V^+ = [[2, 1], [1, 2]]$ $V^- = [[2, 2], [0, 2]]$
6.90232 ^r	$V^+ = [[0, 0, 0, 0], [1, 1, 0, 0], [0, 0, -1, 0], [1, 0, 1, 1]]$ $V^- = [[0, 1, 1, 1], [0, 1, 0, 0], [-1, 0, -1, 1], [0, 0, 0, 1]]$
6.90235	$V^+ = [[-1, 0, 0, 0, 0, -1], [-1, -1, -1, 0, 0, 0], [0, 1, 0, -1, 0, 0], [0, 0, 0, 1, -1, 0], [0, 0, 0, 0, 1, 0], [1, 0, 0, 0, 1, 0]]$ $V^- = [[-1, 0, 0, 0, 0, 0], [-1, -1, 0, 0, 0, 0], [0, 0, 0, 0, 0, 0], [0, 0, -1, 1, 0, 0], [0, 0, 0, -1, 1, 1], [0, 0, 0, 0, 0, 0]]$

TABLE 3. Seifert matrices of almost classical knots.

MATHEMATICS & STATISTICS, McMASTER UNIVERSITY, HAMILTON, ONTARIO
E-mail address: `boden@mcmaster.ca`

URL: `math.mcmaster.ca/~boden`

MATHEMATICS, MONMOUTH UNIVERSITY, WEST LONG BRANCH, NEW JERSEY
E-mail address: `mchristma@monmouth.edu`
URL: <https://micah46.wixsite.com/micahknots>

MATHEMATICS & STATISTICS, McMASTER UNIVERSITY, HAMILTON, ONTARIO
E-mail address: `gaudreai@mcmaster.ca`